ARTICLE

# Functionalized Layered Double Hydroxides for Innovative Applications

Received 00th January 20xx,
Accepted 00th January 20xx

DOI: 10.1039/x0xx00000x

Minwang Laipan,[a,b,c,d] Jingfang Yu,[e] Runliang Zhu,[c,d,*] Jianxi Zhu,[c,d] Andrew T. Smith,[a,b] Hongping He,[c,d] Dermot O'Hare,[e,*] Luyi Sun[a,b,f,*]

Two-dimensional layered double hydroxides (LDHs) are currently a topic of significant interest due to their extraordinary physiochemical properties. LDHs are potentially useful in a wide range of applications, particularly in environmental, energy, catalysis, and biomaterials related fields. Despite the unique intrinsic properties of LDHs, various functionalization strategies have been applied to LDHs that yield even more exciting performance opportunities, offering guides to design novel functional nanomaterials. In this review, we address how these strategies can improve the various properties of LDHs. We provide an overview of the functionalizing strategies of intercalation, surface modification, hybridization, layered compositions regulation, size and morphology control, and defect creation. These strategies contribute significantly to the enhancement of the performance of LDHs, across a diverse range of areas such as adsorptive, catalytic, electronic, electrochemical, and optical. As a result, functionalized LDHs exhibit great potential in a wide range of applications in the environmental and energy domains. We have comprehensively highlighted their emerging potential in the environmental, energy, catalysis, and biomaterials related fields, including heavy metal removal, radionuclide capture, organic contaminants purification, oil pollution elimination, hydrogen generation, supercapacitors, batteries, solar cells, catalysis, and biomaterial fabrication.

## 1. Introduction

Two-dimensional (2D) layered materials are currently a topic of significant interest due to their extraordinary physiochemical properties.[1] Their unique anisotropic structural characteristics make them potentially useful in a wide range of applications, such as optoelectronics, photonics, catalysis, piezoelectric devices, environmental pollution control, energy storage and conversion, and biomaterials.[1-3] Layered double hydroxides (LDHs), previously known as anionic clays, are one family of 2D materials that have attracted significant interest in recent years. LDHs comprise of positively charged edge-shared octahedral coordinated metal hydroxide layers sandwiched by charge compensating interlayer anions with optional solvation eg. water. The general formula of an LDH is $[M^{a+}_{1-x}M'^{b+}_{x}(OH)_2]^{y+}[A^{c-}_{y/c}]^{y+}\cdot zH_2O$ ; $y = a(1-x) + bx - 2$; $A^{c-}$ is an interlayer anion; M and M' are metal cations. Most frequently LDHs conform to the formula $[M^{2+}_{1-x}M'^{3+}_{x}(OH)_2]^{x+}[A^{c-}_{x/c}]^{x+}\cdot zH_2O$ (where $M^{2+}$ and $M'^{3+}$ are divalent and trivalent metal cations typically of $Mg^{2+}$ and $Al^{3+}$ respectively; $A^{c-}$ are inorganic or organic anions) (Figure 1).[4, 5,6, 7] In a few special cases the $M^{2+}$ site can be substituted by $Li^{+}$ and the $M^{3+}$ site can be substituted by $M^{4+}$ cations.[8] In this review, an LDH containing the metal components, $M^{1/2+}$ and $M'^{3/4+}$ are abbreviated as MM'-LDH. LDHs became the focus for both fundamental research and practical applications due to their unique structures, tunable chemical compositions, and a wide variety of material properties.[6, 9-13] Despite the unique intrinsic properties of LDHs, various functionalization strategies have been applied to LDHs that yield even more exciting performance opportunities. That is, functionalization can drastically improve the performance of LDHs or develop new properties for use in a wide range of applications. For instance, the fabrication of three-dimensional hierarchical nano-architecture of an NiFe-LDH remarkably facilitated its rate of electron transport and channel diffusion for catalytic water splitting.[14] Hybridizing with conductive textile fibers made NiCo-LDH a promising candidate for high-performance pseudocapacitors.[15] Intercalation of polysulfide developed the potential of MgAl-LDH for highly selective and efficient capture of radionuclide, e.g., uranium.[3] Hybridization of LDHs with semiconductors to form heterojunction can markedly inhibit the recombination of charge carriers, and thus significantly enhance photocatalytic activity.[16, 17]

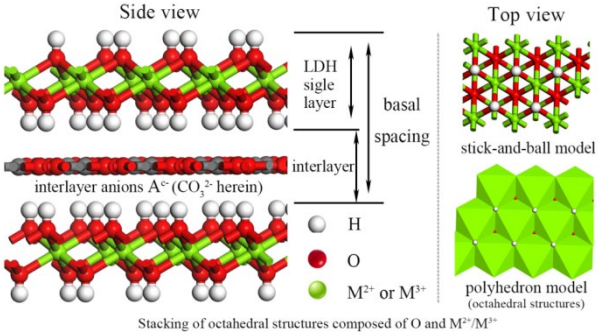


Stacking of octahedral structures composed of O and $M^{2+}/M^{3+}$

[a] Polymer Program, Institute of Materials Science, University of Connecticut, Storrs, CT 06269, USA.
E-mail: luyi.sun@uconn.edu
[b] Department of Chemical and Biomolecular Engineering, University of Connecticut, Storrs, CT 06269, USA
[c] CAS Key Laboratory of Mineralogy and Metallogeny/Guangdong Provincial Key Laboratory of Mineral Physics and Materials, Guangzhou Institute of Geochemistry, Chinese Academy of Sciences, Guangzhou 510640, China.
E-mail: zhurl@gig.ac.cn
[d] Institutions of Earth Science, Chinese Academy of Sciences
[e] Chemistry Research Laboratory, Department of Chemistry, University of Oxford, 12 Mansfield Road, Oxford, OX1 3TA, UK.
E-mail: dermot.ohare@chem.ox.ac.uk
[f] Department of Biomedical Engineering, University of Connecticut, Storrs, CT 06269, USA.

Figure 1. Representative structure of an LDH; $[M^{2+}_{1-x}M'^{3+}_{x}(OH)_2][A^{c-}_{x/c}]$, where $M^{2+}$ and $M'^{3+}$ are divalent and trivalent metal cations, respectively; $A^{c-}$ is an interlayer anion.

Functionalization of LDHs is a process involving the control and manipulation of their surface zone, shape, size, and composition to activate them, or introduction of foreign species or defects on LDHs to enhance or create new functions.[1, 9, 18-20] The modification of surface zone includes intercalation of functional species and alteration of surface functional groups. Introduction of foreign species emphasizes anchoring functional substances onto the surface of LDHs to generate LDH-based hybrids. Apart from the modification of surface zone and introduction of functional species, LDHs can also be functionalized by manipulation of layer composition including the type, ratio, and chemical valence of the metal components, by regulation of the size and morphology of LDHs, and by creation of defects resulting from surface and layered composition regulation. Herein, we summarize the common functionalization strategies that have been developed for LDHs in the following major categories: (1) intercalation,[2, 3] (2) surface modification,[21, 22] (3) hybrid assembly,[23, 24] (4) layer composition tuning,[25, 26] (5) size and morphology regulation,[14, 27] (6) defect introduction,[26, 28] among others. Each of these functionalization strategies demonstrates that with the appropriate modification LDHs can deliver novel and/or enhanced features, e.g., enhanced photoelectronic,[23, 29] magnetic,[30] catalytic,[29, 31, 32] and energy storage[15, 33, 34] properties, offering unique perspectives and advantages for both fundamental and applied research.

The fundamentals why these strategies can effectively functionalize LDHs are outlined in this review article. For example, the reasons that intercalation is such a versatile and effective approach in tuning the properties of LDHs are: (1) intercalation provides the highest possible doping and/or phase change to the pristine LDHs; (2) the intercalation process, and the concomitant changes in the properties of LDHs is typically reversible; (3) intercalation is controllable; (4) changes in intercalated LDHs during material preparation can be monitored *in situ* and in real time; (5) intercalation can induce structural changes, such as lattice expansion or even phase changes, for improved or new physiochemical properties; (6) intercalation adds a new degree of freedom for tuning LDHs, which can be combined with other modification methods.[1] The modification of surface functional groups of LDHs can be one of the most common strategies in altering the surface properties of LDHs, because the introduction of foreign functional groups renders LDHs to possess different or enhanced functions. For instance, the introduction of amine terminal groups onto MgAl-LDH makes the MgAl-LDH a potential biomaterial without causing any hemolysis,[35, 36] and enhances its functions in the environmental field.[37] The reason that the introduction of functional materials onto LDHs can alter the properties of LDHs is ascribed to the fact that it can combine the strength of each component in the structure and functions. I n addition, the components in hybrids may even generate synergies, which will result in the enhancement of the properties.[19, 20, 34 23, 24, 38] For example, in the electrochemical field, LDHs have been reported to be promising electrode materials for the next-generation supercapacitors, but the relatively low conductivity of LDHs constrains their performance.[39, 40] It's suggested that the electrochemical properties of LDHs can be further improved by the hybridization with conductive materials.[29] This is because the conductive materials, e.g., graphene, can significantly enhance the electrical conductivity and accelerate the electron transfer, resulting in excellent charge and discharge capability.[41-45] Many other reasons for the enhanced or newly created functions of LDHs produced by various functionalization strategies are summarized in Section 2.

In this review, we focus on the functionalization strategies for LDHs, and highlight the significance of functionalization in tuning the physiochemical properties of LDHs and their subsequent applications particularly in the environmental, energy, catalysis, and biomaterials sectors. We also provide some insights into the challenges and future opportunities of LDHs.

## 2. Strategies to functionalize LDHs

In general, functionalization of LDHs can be achieved by modifying their surface zone, assembling hybrids, and regulating layer composition, size and morphology. The modification of surface zone includes intercalation of functional species and alteration of surface functional groups. Hybrid assembly emphasizes anchoring functional substances onto the surface of LDHs to generate LDH-based hybrids. The assembly usually occurs at the interface between LDHs and the loaded functional substances. Manipulation of layer composition focuses on the regulation of type, ratio, and chemical valence of the metal components. The size and morphology section highlights the impact of size and morphology on the properties of LDHs. Apart from the above aspects, other factors such as creation of defects resulted from surface and layered composition regulation can also be utilized to functionalize LDHs.

### 2.1 Intercalation

The phenomenon of intercalation was first discovered *ca*. 600-700 A.D. in China.[46] At that time, alkali metal ions were intercalated into natural minerals, such as kaolin, to make porcelain.[47] The first intercalation phenomenon in the literature was reported by Schafhäutl in 1840, in which the authors attempted to dissolve graphite in sulphuric acid.[48] The modern era of intercalation research was initiated in 1926 by Fredenhagen *et al.*, in which the uptake of potassium vapor into graphite was reported.[49] Over the subsequent decades, intercalation strategies for 2D materials have significantly advanced and various mechanisms have been clarified.[18, 50-63] Exploring the benefits of intercalation in 2D materials for various applications remains a very active contemporary field of research.

The intercalation of 2D LDHs is a process of inserting a foreign species between the edge-shared metal hydroxide layers of the LDHs (Figure 2). In many instances, intercalation can lead to drastically improved performance for the LDHs. For example, incorporation of homogeneous catalysts (e.g., inorganic anions, organic acid/base, organic complexes) into LDH interlayer space offers the chance to heterogenize the homogeneous reaction process over LDH-based catalysts with enhanced lifetime and thermal stability, as well as facile separation/purification.[9] Intercalation can also make LDHs more favorable for the use of energy storage and conversion. In one example, the intercalation of bistrifluoromethane sulfonamide into galleries of CoTi-LDH endowed CoTi-LDH with the ability in making up low-overpotential Li-$O_2$ batteries with superior cycling stability.[64] Herein, we summarize some common LDHs and intercalants reported in recent years, and the benefits of the intercalation in improving various performances of LDHs (Table 1). The data suggests that different combinations of LDHs and intercalants can offer different

 

performances, and intercalation is indeed a promising means to functionalize LDHs and to expand their applications. The reasons that intercalation is such a versatile and effective approach in tuning the properties of 2D LDHs are: (1) intercalation provides the highest possible doping and/or phase change to the pristine LDHs; (2) the intercalation process, and the concomitant changes in the properties of LDHs is typically reversible; (3) intercalation is controllable; (4) changes in intercalated LDHs during material preparation can be monitored *in situ* and in real time; (5) intercalation can induce structural changes, such as lattice expansion or even phase changes, for improved or novel physiochemical properties; (6) intercalation adds a new degree of freedom for tuning LDHs, which can be combined with other modification methods.[1]

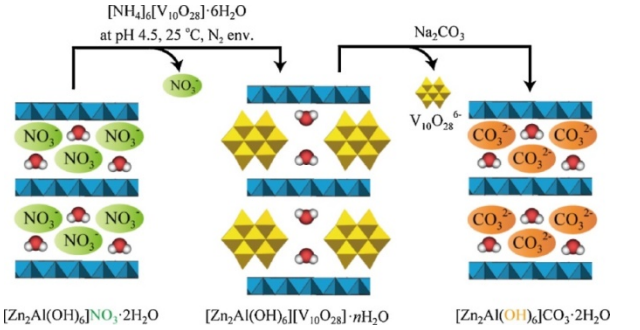


Figure 2. Schematic illustration of the intercalation of ZnAl-LDH.[65] Reproduced with permission from ref. [65], Copyright 2014, Elsevier.

Table 1. Representative examples reported in recent years of LDH intercalation, and the benefits of the intercalation in improving various performances of LDHs.

| LDH | Intercalant | Performance vs. the pristine LDH | Ref. |
|---|---|---|---|
| MgAl | Polysulfide | Highly selective and efficient for radionuclide ($UO_2^{2+}$) sequestration | 3 |
| MgAl | $MoS_4^{2-}$ | Highly selective and efficient for heavy metals and radionuclides removal; 5-8 folds increase of the capture capacities | 2, 66 |
| MgAl | Hydroxyl ammonium ionic liquids | ~6 folds higher adsorptive capacity towards organic contaminants | 67 |
| MgAl | $Fe(CN)_6^{4-}/S^{2-}$ | Endowed LDH with an ability of rapid detection of heavy metal ions | 68 |
| MgAl | Keggin polyoxometalate | Highly efficient catalytic activity; produced the highest turnover number reported in Knoevenagel condensation of benzaldehyde with ethyl cyanoacetate | 69, 70 |
| Silylated MgAl | $MnO_2$ nanowires | High catalytic activity, stability, and reusability | 71 |
| MgAl | $MnO_2$ | Enhanced electrocatalytic activity; excellent stability, selectivity, and reproducibility | 72 |
| MgAl | Ruthenium polypyridine complex | High thermal and photo stability; enhanced luminescence efficiency and lifetime | 73 |
| MgAl | Decavanadate | Enhanced corrosion-resistant properties, especially long-term corrosion resistance | 74 |
| MgAl | $CO_3^{2-}/NO_3^-$ | Tunable electronic transport properties by changing intercalated ions | 75 |
| NiCr | Diphenylamine-4-sulfonate | Highly selective and efficient for heavy metal removal | 76 |
| NiFe | Cobalt | Significantly enhanced catalytic activity for water splitting; long term stability | 77 |
| NiCo | n-alkylsulfonate anions | Tunability of magnetic properties, enhanced coercivity | 78 |
| NiCo | Ethylene glycol | Ultrahigh specific capacitance and excellent cycling stability | 79 |
| NiMn | $MnO_2$ | Greatly improved supercapacitor behavior | 80 |

### 2.2 Surface modification

Modification and control of surface properties of LDHs are of crucial importance in the functionalization of LDHs. There are numerous studies focusing on the surface modification of LDHs by hybridizing functional materials onto the surface of LDHs. For example, surfactants are the most popular functional species to be anchored onto the LDH surface to functionalize an LDH.[18, 19] In this section, we focus on the regulation of the properties of LDHs by the introduction of various functional groups.

The modification of surface hydroxyl groups of LDHs can be one of the most common strategies in altering the surface properties of LDHs. For example, Oh *et al*. modified the surface hydroxyl groups of MgAl-LDH by grafting aminopropyltriethoxysilane, which introduced amine terminal groups onto the surface of MgAl-LDH without affecting the LDH layered structure (Figure 3a).[81] The amine terminal groups could be utilized as an active site for further modification to render MgAl-LDH as an effective drug-delivery carrier.[81] Hu *et al*. found that the functionalized MgAl-LDH with amine terminal groups (functionalized through a three-step surface grafting process) possessed enhanced blood compatibility, which made it a potential biomaterial without causing any hemolysis.[35, 36]. Besides the applications in the medical field, amine groups functionalized LDHs can also be used in the environmental field. For example, Ezeh *et al*. found that after amine modification, MgAl-LDH

presented an enhanced physical adsorption of $CO_2$, and with an increase of amine loading, the adsorption of $CO_2$ was further enhanced.[37] In another example, Li et al. introduced various functional groups including phenolic hydroxyl groups, alcoholic hydroxyl groups, and carboxyl groups onto the surface of ZnAl-LDH by loading fulvic acid.[82] The fulvic acid anchored ZnAl-LDH showed a great ability to simultaneously remove organic dyes and heavy metal cations. In addition to the functional groups derived from organic compounds, functional groups from inorganic substances can also functionalize LDHs. For instance, Lima et al. prepared fluorinated MgAl-LDH by using $NaAlF_6$, and found that the introduction of surface F terminal groups onto MgAl-LDH could significantly modify the physicochemical, thermal, and adsorptive properties.[83]

Apart from the above discussed functional groups, many other groups have been grafted onto the surface of LDHs, such as epoxide group, disulfide bonds, Br groups, and silanol groups,[7, 18, 36] which led to remarkable improvement in a range of physical properties of the LDHs.

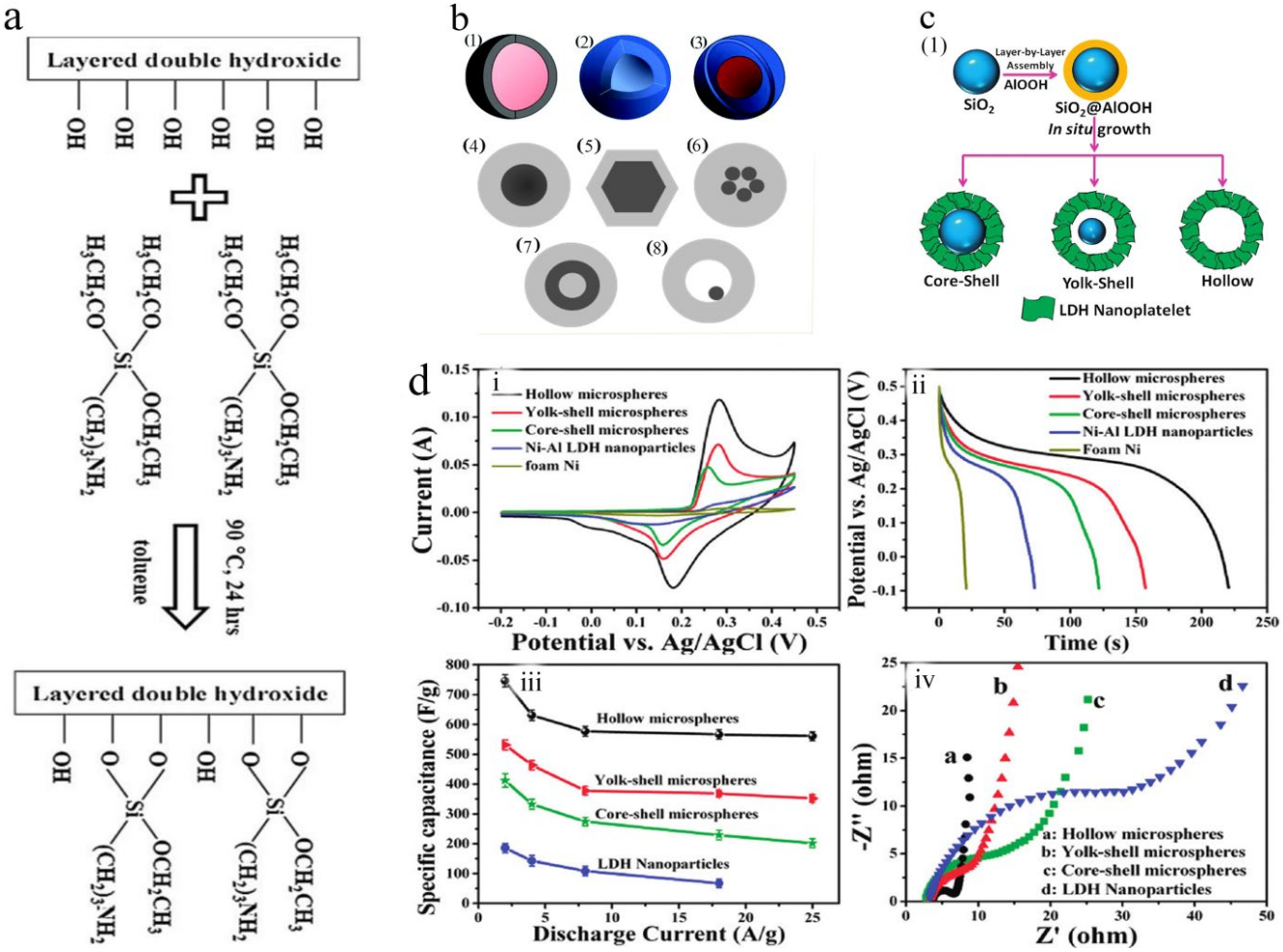


Figure 3. (a) Schematic illustration of aminopropyltriethoxysilane (amine terminal groups) grafting onto the surface of MgAl-LDH.[81] Reproduced with permission from ref.[81], Copyright 2009, WILEY-VCH Verlag GmbH & Co. KGaA, Weinheim. (b) Schematic illustration of (1) core-shell; (2) hollow core-shell; (3) yolk or rattle core-shell nanostructures; (4) spherical core-shell nanoparticles; (5) hexagonal core-shell nanoparticles; (6) multiple small core materials coated by single shell material; (7) nanomatryushka material; (8) movable core within hollow shell material.[84] Reproduced with permission from ref. [84], Copyright 2016, The Royal Society of Chemistry. (c) Schematic illustration of preparation of LDH microspheres with tunable interior architecture from core-shell to hollow structure. (d) Cyclic voltammograms (CVs) curves (i); galvanostatic (GV) discharge curves (ii); current density dependence of the specific capacitance (iii); Nyquist plots of the electrochemical impedance spectroscopy for the hollow, yolk-shell, core-shell LDH microspheres, and LDH nanoparticles (reference sample) (iv).[85] Reproduced with permission from ref. [85], Copyright 2012, American Chemical Society.

### 2.3 Hybridization

The combination of two or more distinct properties into a unique composite is an exciting direction for the fabrication of novel multifunctional materials. Construction of LDH-based hybrids, especially one with a nanostructure, by interacting LDHs with other materials (e.g., silica nanoparticles, magnetic nanoparticles, semiconductors, rare earth and noble metal elements), is an emerging active research vector which may serve various fields, such as environmental remediation, energy conversion and storage.[23, 24, 38] The introduction of functional materials onto LDH can alter the properties of LDHs, offering various enhanced or new functions to LDHs. Hybrid assembly provides the advantages of combining the strength of each component in the structure and functions. In addition, the components in hybrids may generate synergies. The resultant

 

hybrids may exhibit new properties depending on the interactions between the different components. Herein, we mainly highlight the construction of LDH-based hybrids by the fabrication of core-shell structure and the loading of conductive materials, semiconductors, and rare earth elements or noble metals onto LDHs to enhance or extend the functions of LDHs. Notably, some LDH-based hybrids can be grouped into different sections. These materials will be discussed only in one of the sections below.

**2.3.1 Introduction of a "core" or "shell"**

The terminology of "core-shell" was first adopted in the early 1990s when researchers attempted to synthesize concentric multilayer semiconductor nanoparticles to improve the property of semiconductor materials.[86] Figure 3b shows different types of core-shell structures. The general concept of core-shell presents two materials with two functions in one structure (Figure 3b-1). When the core is removed, hollow core-shell structural material will be created (Figure 3b-2). And by combining the above two types of core-shell structures, the yolk or rattle core-shell architecture which has a core@void@shell configuration (Figure 3b-3) is generated.[86] Generally, core-shell nanoparticles are well-known for better stability, for being able to protect the core material from the surrounding environment, for improved physiochemical properties, for improved semi-conductive properties, for easy biofunctionalization. The shell could change the functions and properties of the original core,[84] and the core could also modify the functions and properties of the original shell.[87] In other words, the core/shell can exhibit new chemical or physical properties with shell/core formation. In addition, core-shell composites may have properties that are synergistic between the core and the shell and/or offer new properties depending on the interactions between the core and the shell.[87, 88]

Thanks to the above highlighted merits, the construction of core-shell composites has become an effective avenue to functionalize LDHs. For instance, to enhance the supercapacitor behavior of NiAl-LDH, Shao *et al*. fabricated core-shell LDH microspheres with tunable interior architecture using $SiO_2$ as a core.[85] Via the regulation of interior architecture, core-shell, hollow core-shell, and yolk core-shell types of NiAl-LDHs were produced (Figure 3c), and variations in specific surface area and pore-size distribution were achieved. Moreover, the prepared core-shell microspheres, especially the hollow ones, exhibited excellent pseudocapacitance performance, including high specific capacitance and rate capability, high charge/discharge stability, and long-term cycling life (Figure 3d). The improvement of the supercapacitor performance of NiAl-LDH was due to the greatly improved faradaic redox reaction and mass transfer. In another example, Han et al. used CoAl-LDH as the core to produce flexible CoAl-LDH@poly(3,4-ethylenedioxythiophene) core-shell nanoplatelets for high-performance energy storage.[87] The synthesized material exhibited high specific capacitance, excellent rate capability, and long-term cycling stability, which were superior to those of the conventional supercapacitors and the CoAl-LDH without the shell of poly(3,4-ethylenedioxythiophene). The largely enhanced pseudocapacitor performance of the prepared material was related to the synergistic effect of its individual components: the LDH nanoplatelet core provided abundant energy-storage capacity, while the highly conductive poly(3,4-ethylenedioxythiophene) shell and the porous architecture facilitated the electron/mass transport in the redox reaction. LDH-based core-shell materials have growing applications because of the multifunctionality that is achieved through the tailoring of core/shell materials. Table 2 summarizes some representative LDH-based core-shell composites in the past three years and the significance of fabrication of a core-shell structure. Clearly, novel physiochemical properties, such as medical, magnetic, catalytic, electrochemical, and electronic characteristics can be imparted to LDHs through the formation of a core-shell structure.

Table 2. Representative LDH-based core-shell hybrids reported in the past three years.

| Core/Shell | Synthesis method | Performance vs. the pristine LDH | Ref. |
|---|---|---|---|
| $Fe_3O_4$/CuAl-LDH | Hydrothermal and co-precipitation | Endowed magnetism; endowed high sensitivity, good reproducibility, and long-term stability as electrochemical sensors; endowed real-time monitoring for live cancer cells | 89 |
| $Fe_3O_4$/enrofloxacin intercalated MgAl-LDH | Delamination–reassembly | Endowed magnetism; enhanced stability; potential magnetic targeting drug delivery-controlled-release system | 90 |
| $Fe_3O_4$/(Zn, Mg, Ni)Al-LDH | Co-precipitation | Endowed high superparamagnetism for easy separation | 91 |
| $Co_3O_4$/NiCoAl-LDH | Two-step hydrothermal synthesis | Enhanced electrochemical performance: exhibited high specific capacitance (1104 F $g^{-1}$ at 1 A $g^{-1}$), adequate rate capability and cycling stability (87.3% after 5000 cycles) | 92 |
| $NiCo_2O_4$/NiCoAl-LDH | Hydrothermal synthesis and a step-by-step in situ structure fabrication | Enhanced specific capacitance of 1814.24 $Fg^{-1}$ at a current density of 1 $Ag^{-1}$ and 93% retention after 2000 cycles at 10 $Ag^{-1}$. | 93 |
| ZnO/CuZnAl-LDH | Deposition-Precipitation | Enhanced activity in photoreduction of $CO_2$ to hydrocarbons | 94 |
| CuO/CoFe-LDH | Calcination and electrodeposition | Largely improved specific capacitance, high rate capability and long cycling lifespans; exhibited excellent supercapacitive performances with a high energy density (1.857 mWh $cm^{-3}$) and long-term cycling stability (99.5% device capacitance retention after 2000 cycles) | 95 |
| $TiO_2$/CoNi-LDH | Electrodeposition | Remarkably enhanced performance for photoelectrochemical water splitting | 96 |
| ZnO and CdS/CoNi-LDH | Electrodeposition | Efficient solar water oxidation | 97 |

| | | | |
|---|---|---|---|
| $Cu_2O$/ZnCr-LDH | *In situ* crystallization-selective etching method | Largely enhanced visible-light-driven water splitting efficiency: with a $H_2$ and $O_2$ production rate of 0.90 and 0.44 μmol $h^{-1}$, respectively, without any sacrificial agent and co-catalyst, which is among the highest of the reported photocatalysts under the same conditions | 98 |
| $MnO_2$/NiFe-LDH on Ni foam | Hydrothermal | Enhanced supercapacitor performance: high capacitance of 4274.4 mF $cm^{-2}$ at 5 mA $cm^{-2}$ and a capacitance retention of 95.6% after 1000 cycles from a traditional three-electrode system | 99 |
| $WO_3$/NiFe-LDH | Hydrothermal | Enhanced photoelectrochemical water splitting | 100 |
| $BiVO_4$/(Ni,Co)Fe-LDH | Electrodeposition | Greatly enhanced photocatalysis for the oxygen evolution reaction | 101 |
| $SiO_2$/DNA intercalated NiIn-LDH | Layer-by-Layer assembly | Low infrared emissivity | 102 |
| $SiO_2$/MgAl-LDH | Co-precipitation | Tunable size and morphology | 103 |
| Zeolites/MgFe-LDH | Co-precipitation | Solved the problem of the application of powdered LDH in constructed rapid infiltration system | 104 |
| Nickel phosphide /NiCo-LDH | Phosphorization of Ni foam and subsequent electrodeposition | Significantly enhanced electrochemical performances: high specific capacitance, and excellent cycling stability | 105, 106 |
| Fe/MgAl-LDH | Co-precipitation | High adsorption of organic contaminants | 107 |
| Cu/CoFe-LDH | Electrodeposition | Afforded small overpotentials of 171 mV for the hydrogen evolution reaction and 240 mV for the oxygen evolution reaction at a current density of 10 mA $cm^{-2}$, along with Tafel slopes of 36.4 and 44.4 mV $dec^{-1}$ for the hydrogen evolution reaction and oxygen evolution reaction, respectively | 108 |
| Cu/NiFe-LDH | Electrodeposition | Exhibited outstanding oxygen evolution reaction activity as well as excellent hydrogen evolution reaction performance in an alkaline medium | 14 |
| Porous graphitized carbon/NiFe-LDH | One-step hydrothermal | Excellent oxygen evolution reaction properties with a low onset potential and a lower overpotential; superior catalytic activity; enhanced electrocatalyst | 109 |
| Hollow carbon nanospheres /NiCo-LDH | Hydrothermal | Remarkable electrochemical properties: much higher of the specific capacitances and outstanding rate capability | 110 |
| Graphene-encapsulated carbon/NiAl-LDH | Electrostatic-induced assembly | Exhibited high specific capacitance; high energy density with an excellent rate capability as well as a robust long-term cycling stability | 111 |
| ZnAl-LDH/ZIF-8 (one of the zeolitic imidazolate frameworks) | *In situ* grown on the ZnAl-LDH | Enhanced $CO_2$ capture | 112 |
| NiCo-LDH/reduced graphene oxide | One-pot hydrothermal method | Significantly enhanced electrochemical performance: high performance asymmetric supercapacitors with remarkable cycling stability | 113 |
| NiCoAl-LDH /carbonaceous aerogel | Hydrothermal | High specific capacitances; excellent cycling stability | 114 |
| Carborane intercalated MgAl-LDH /magnesium ferrite | Direct mixing | Potential to be used in Boron Neutron Capture Therapy (BNCT) and magnetically targeted-BNCT applications | 115 |
| NiFe-LDH /NiFe-borate | Hydrothermal | Produced highly efficient water oxidation electrocatalysis in near-neutral media with a strong electrochemical durability | 116 |
| NiFe-LDH/Au nanoarrays on Ni foam | Hydrothermal and chemical deposition | Exhibited superior catalytic activity and durability toward oxygen evolution reaction in 30 wt % KOH | 117 |

According to the previous studies, a number of factors are important role in deciding the physical and chemical properties of core-shell materials, such as (a) ligand effect, which involve the interactions between the core and the shell due to atomic proximity affecting the charge transfer between the components; (b) ensemble effect, which is governed by the material's adsorption on the surface due to the presence of distinct atomic groups, and (c) geometric effect, originating from the difference in reactivity of the surface atoms because of their three dimensional structural constraints (e.g., surface strain).[88]

### 2.3.2 Hybridization with conductive materials

LDHs are emerging as potential candidates in electrochemical, photo-electrochemical, and photochemical applications due to the facile tunability of their chemical composition, many transition metal ions across a range of oxidations states possess ionic radii that can be accommodated within the octahedral sites. Their electrochemical, photo-electrochemical and photochemical properties can be further improved by the hybridization with conductive materials.[29] In the electrochemical field, for example, LDHs were reported to be promising electrode materials for the next-generation supercapacitors.[39, 118] However, the relatively low conductivity of LDHs constrains electron transfer, resulting in poor charge and discharge capability that adversely affects the performance of electrode materials.[39, 40] Hybridization LDHs with conductive materials has been demonstrated to be a feasible and effective approach to enhance the electron conductivity.[119-121] For instance, Zhang *et al*. designed and synthesized a hybrid of CoAl-LDH and graphene, they found that the loading of conductive graphene endowed CoAl-LDH with a high specific capacitance that was much higher than the pure CoAl-LDH. In addition, the obtained hybrid showed a high cycle stability of 93.9% of the specific capacitance retained at 3 $Ag^{-1}$ after 2000 cycles.[39] The improved electrochemical performance benefited from the anchoring electroactive graphene onto the surface of LDH. Liu et al. anchored conductive carbon nanoparticles onto

 

the surface of NiAl-LDH, and manifested the resulting supercapacitor to exhibit excellent capacitive performance, including a high specific capacitance, good cycling capability and high energy density. The enhanced electrical conductivity that resulted from the incorporation of carbon nanoparticles contributed to the improved capacitance and rate capability.[122] Yang *et al.* designed a graphene oxide (GO) surface-confined strategy to fabricate NiCo-LDH-graphene nanosheet composites (Figure 4). By this strategy, ultrathin 2D nanosheets with a thickness of 1.7-1.8 nm that are duplicated from the GOs in terms of both the lateral dimensions and the shape can be prepared. The as-obtained NiCo-LDH-graphene nanosheets exhibited a superior electrocatalytic activity for oxygen evolution reaction, evidenced by a small overpotential of 0.337 V (@10 $mA \cdot cm^{-2}$ in 0.1 M KOH electrolyte), and a high charge storage capability of 1489 $F \cdot g^{-1}$ as electrodes for supercapacitors. The authors pointed out that the relatively wide interlayer distance, ultrathin and highly tortuous structures, large specific surface area, multilevel pore structure, and high electrical conductivity benefited from graphene resulted in the high activity.

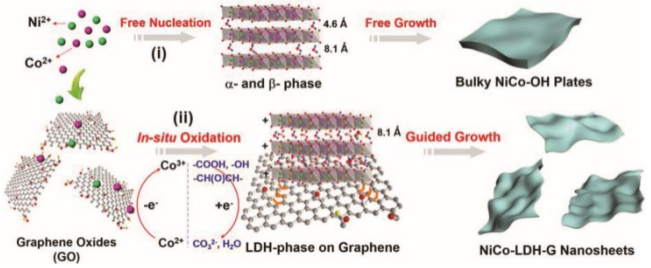


Figure 4. Schematic of the fabrication routes of the NiCo-LDH-graphene nanosheets (NiCo-LDH-G). i) Growth process of NiCo-hydroxide (NiCo-OH) in the absence of GO, leading to the bulky and rigid NiCo-OH plates with the main interlayer spacing of ≈4.6 Å; ii) GO surface-guided growth of NiCo-LDH nanosheets, yielding ultrathin and highly tortuous NiCo-LDH-G nanosheets with an interlayer distance of ≈8.1 Å. Reproduced with permission from ref.[123], Copyright 2018, WILEY-VCH Verlag GmbH & Co. KGaA, Weinheim

In photocatalysis, hybridization of LDHs with conductive materials brings similar benefits. The ease in electron-hole recombination for many LDH photocatalysts restrains their applications in photocatalysis. The hybridization with electron accepting species provides a powerful approach to further enhance the photocatalytic efficiency of the LDH material by the timely conduction of electrons to prolong the lifetime of electron and hole. Gunjakar *et al*. assembled a highly effective photocatalyst by combining ZnCr-LDH with graphene nanosheets (Figure 5a).[29] The coupling of graphene with ZnCr-LDH gave a remarkable depression of the photoluminescence signal, and an unusually high photocatalytic activity for visible light-induced $O_2$ generation with a rate of ca. 1.20 mmol $h^{-1}g^{-1}$, which was far superior to that of the pristine ZnCr-LDH (ca. 0.67 mmol $h^{-1}g^{-1}$; note that pristine ZnCr-LDH is one of the most effective visible light photocatalysts for $O_2$ production with an unusually high quantum efficiency of 61% at 410 nm wavelength). The loading of graphene gave rise to a remarkable depression of electron-hole recombination by the timely conduction of electrons. Figure 5b-2 shows a schematic illustration of electronic coupling between ZnCr-LDH and graphene, showing how graphene takes effect.

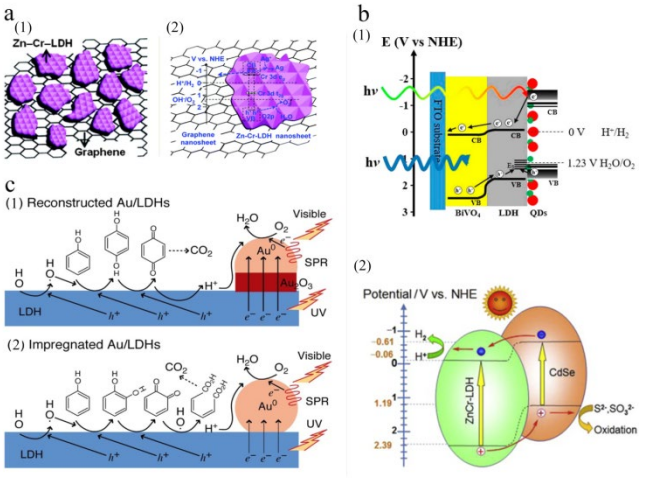


Figure 5. (a): (1) Structural model for the self-assembled nanohybrids of ZnCr-LDH-graphene; (2) schematic illustration of electronic coupling between ZnCr-LDH and graphene under light irradiation.[29] Reproduced with permission from ref.[29], Copyright 2013, The Royal Society of Chemistry; (b): (1) schematic illustration of $BiVO_4$/CoAl-LDH heterojunction in electron (-) and hole (+) separation and transport under light irradiation,[124] Reproduced with permission from ref.[124], Copyright 2016, American Chemical Society; (2) schematic illustration of CdSe/ZnCr-LDH heterojunction in electron (-) and hole (+) separation and transport under visible light irradiation,[125] Reproduced with permission from ref.[125], Copyright 2015, Elsevier; (c) proposed reaction mechanism (charge transfer between gold nanoparticles and ZnAl-LDH and surface plasmon resonance (SPR) effect of gold) of photocatalytic phenol decomposition on gold species formed on ZnAl-LDH: (1) $Au^{3+}$-$Au^0$-ZnAl-LDH, and (2) $Au^0$-ZnAl-LDH.[126] Reproduced with permission from ref.[126], Copyright 2016, Elsevier.

Table 3 summarizes the LDH-based hybrids anchored with various conductive materials in recent years. LDHs containing $Ni^{2+}$, $Co^{2+/3+}$, $Fe^{2+/3+}$, $Mn^{2+/4+}$, $Zn^{2+}$, $Ti^{4+}$, and $Al^{3+}$ are the most frequently studied in the electrochemical field, carbon-based materials and metals such as nickel are the most common conductive materials hybridized with LDH. Clearly, anchoring conductive materials with LDH is a promising avenue to functionalize LDH and expand their application as functional electronic materials.

Table 3. Representative LDH-based hybrids anchored with conductive materials in recent years.

| LDH | Anchoring materials | | Performance vs. pristine LDH | Ref. |
|---|---|---|---|---|
| | material | Type | | |
| NiCo | Reduced graphene oxide | Conductive material | Greatly enhanced rate of electron and mass transfer; exhibited excellent supercapacitive properties: high specific capacitance, extraordinary rate capability, and good cycling stability | 111 |
| NiCo | Carbon nanofibers | Conductive material | Provided not only more active sites for electrochemical reaction but also more efficient pathways for electron transport; enhanced supercapacitors performance | 112 |
| NiCo | Nitrogen-Doped Carbon Nanofiber | Conductive material | Exhibited significantly enhanced specific capacitance and excellent cycling stability | 113 |
| NiCo | Nickel foam | Conductive material | Displayed a high specific capacitance and a unique cyclability | 114, 115 |
| NiCo | Nickel foam and reduced graphene oxide | Conductive material | Exhibited an enhanced specific capacitance, excellent rate capability, and long cyclic life | 116 |
| NiCoFe | Carbon nanofibers and activated carbon | Conductive material | Higher specific capacitance and rate capability; excellent long-time cycle life | 117 |
| NiFe | Graphene oxide | Conductive material | Excellent electrocatalyst for oxygen evolution reaction; exhibiting small overpotential and low Tafel slope | 118, 119 |
| NiFe | Carbon nanotubes | Conductive material | Achieving stable and efficient water oxidation | 120 |
| NiFe | Reduced graphene oxide | Conductive material | Showed superior oxygen evolution reaction performance compared to pristine NiFe-LDH and reference $IrO_2$ | 121 |
| NiFe | Ni | Conductive material | Exhibit a superior specific capacitance of 2708 $Fg^{-1}$ at 5 $Ag^{-1}$ | 122 |
| NiAl | Au, single-walled carbon nanotubes, and graphene | Conductive material | Enhanced electrical conductivity and more electron transfer passages; showed good reproducibility, repeatability, stability, and anti-interference property as non-enzymatic sensor | 123 |
| NiAl | Carbon nanotubes | Conductive material | Carbon nanotubes improved the electrical conductivity and decreased the electrochemical polarization of the composite; much better electrochemical performance than pure NiAl-LDH | 124, 125 |
| NiAl | Nickel foam | Conductive material | Enhanced electrochemical performance: higher specific capacity and cycling stability than those of NiAl-LDH | 126 |
| NiAl | Reduced graphene oxide | Conductive material | Enhanced supercapacitor performance | 127 |
| NiAl | Nickel foam and graphene | Conductive material | Resulted in better electrode stability at high current density; exhibited higher energy and power densities; but leading to a decrease in specific capacity and the rate performance of the electrode | 128 |
| NiAl | Carbon cloth | Conductive material | Highly sensitive electrochemical sensors | 129 |
| NiAl | MXenes | Conductive material | Enhanced supercapacitor performance | 130 |
| CoNiAl | Reduced graphene oxide | Conductive material | Enhanced charge conductivity and electrochemical performance | 131, 132 |
| NiMn | Nickel foam | Conductive material | Largely enhanced supercapacitor behavior: high specific capacitance, excellent rate capability, high coulombic efficiency and long-term cycling life | 133, 134 |
| NiMn | Porous carbon | Conductive material | Largely enhanced supercapacitor behavior: much better specific capacitance, and long-term cycling life | 135 |
| NiMn | (Reduced) graphene oxide | Conductive material | Showed much higher efficiency as electrocatalyst, and the overpotential could be decreased to as small as 0.26 V; higher electrochemical activities | 136-138 |
| NiMn CoMn | Reduced graphene oxide | Conductive material | Improved the capacitance and cyclic stability of the hybrid materials | 139 |
| CoAl | 3D graphene | Conductive material | Exhibited excellent catalytic activity and stability for oxygen evolution reaction in alkaline solution, which was comparable or even better than the state-of-art LDH-related oxygen evolution reaction electrocatalysts | 140 |
| CoAl | Graphene | Conductive material | Enhanced capacitive performance for supercapacitors | 105, 141 |
| CoAl | Fluorinated graphene | Conductive material | Enhanced capacitive performance for supercapacitors | 142 |
| CoAl | Reduced graphene oxide | Conductive material | Enhanced electrochemical performance | 143 |
| CoFe | Graphene | Conductive material | Highly efficient electrocatalyst for oxygen evolution reaction; created well-interconnected conductive networks within the electrode matrix, leading to a low overpotential | 144 |
| CoFe | Carbon fiber cloth | Conductive material | Enhanced electrochemical performance; delivered an improved capacitance | 145 |
| ZnTi | C60 | Conductive material | Enhanced photocatalytic activity for organic contaminant degradation | 8 |

#### 2.3.3 Hybridization with semiconductors

Transition metal-containing LDHs have been reported to exhibit highly-efficient catalytic performance, of most note is their activity in water splitting, and oxidation and reduction of environmental contaminants. Although transition metal containing LDHs show high catalytic performance, hybridizing semiconductors onto LDHs can generally further enhance the catalytic activity of LDHs. Taking the application of LDHs in photocatalysis as an example, anchoring semiconductors on LDHs will commonly result in the formation of heterojunction, which can increase the separation efficiency of the excited electrons and holes to improve the photocatalytic activity by inhibiting the recombination of charge carriers (i.e., the photo-generated holes and electrons). For example, Ao *et al*. found that the hybrid of BiOBr and CoNi-LDH exhibited much higher adsorptive and photocatalytic degradation of organic contaminants (organic dyes and phenol) than either BiOBr or CoNi-LDH under UV-light irradiation.[16] The excellent photocatalytic activity is because of the formed heterojunction between the BiOBr and the CoNi-LDH, which inhibits the recombination of charge carriers, and thus more holes or electrons can be captured to induce the photocatalytic reaction. Figure 5b shows schematic illustrations of different types of semiconductor/LDH heterojunctions in electron-hole separation and transport and photocatalytic activity under visible or solar light irradiation.[124, 125] Clearly, the photo-generated electrons and holes can transfer between LDH and the hybridized semiconductors, which are significantly beneficial to the extension of the lifetime of electrons and holes, and thus increasing the photocatalytic activities.

Anchoring semiconductors onto the surface of LDHs can also improve the electrochemical and photoelectrochemical catalytic activity of the LDHs. For instance, Hu *et al*. hybridized $MoS_2$ onto NiCo-LDH and demonstrated a dramatic enhancement of hydrogen evolution reaction kinetics in base media compared to either $MoS_2$ or NiCo-LDH.[159] The resultant $MoS_2$/NiCo-LDH hybrid exhibited extremely low hydrogen evolution reaction overpotential of 78 mV at 10mA/cm$^2$ and a low Tafel slope of 76.6 mV/dec in 1 M KOH solution. Benefiting from the desirable structural characteristics, the $MoS_2$/NiCo-LDH interfaces synergistically favor the chemisorption of H (on $MoS_2$) and OH (on LDH), and can thus effectively accelerate the water dissociation step and the overall hydrogen evolution reaction. Zhang *et al*. hybridized $TiO_2$ with ZnFe-LDH, and found that $TiO_2$/ZnFe-LDH photoanode exhibited a largely enhanced photoelectrochemical water splitting performance.[160] The study revealed that the photogenerated holes of $TiO_2$ tended to travel to ZnFe-LDH, which enhanced the bulk charge separation, and thus the surface water oxidation reaction. Table 4 summarizes the representative LDH-based hybrids anchored with various semiconducting materials, the table highlights that the anchoring of semiconductors significantly enhances the catalytic activities of LDHs.

#### 2.3.4 Hybridization with noble metals or rare earth elements

Table 5 summarizes the noble metals and rare earth elements that have been anchored on LDHs and the impacts these elements have on enhancing the properties of LDHs. Noble metals such as Au, Ag, Pt, Pd, and Ru, and rare earth elements of Ce, Tb, and La are the most prevalent elements to be anchored onto LDHs. Loading noble metals and rare earth elements on LDHs can dramatically improve the photocatalytic performance with enhanced light absorption, charge transport properties, interfacial kinetics,[171] and the adsorptive abilities for reactants.[171, 172] Noble metals and rare earth elements improve the properties of LDHs owing to one or several of the following aspects:[40, 126, 171, 172] (1) noble metals and rare earth elements are electron-abundant species which possess prominent electron donating abilities; (2) noble metals and rare earth elements have strong coordination abilities; that is, when integrated into LDH, they can serve as adsorptive sites; (3) noble metals and rare earth elements can conduct electrons promptly; (4) the loading of noble metals and rare earth elements may create lattice distortions which can be active sites; (5) photoresponsive characteristics, e.g., surface plasmon resonance, of noble metals and rare earth elements. Taking the applications of LDHs in photocatalysis as an example, LDHs have emerged as highly active photocatalysts due to their unique structure, large specific surface area and semiconductive properties. However, the slow interfacial kinetics and fast charge recombination (due to the poor charge mobility) are the major obstacles which limit the performance of LDH-based photocatalysts. Fu *et al*. demonstrated the incorporating terbium onto ZnCr-LDH could significantly inhibit the recombination of photo-induced charge carriers and increase the charge injection efficiency simultaneously, and thus largely enhanced the visible light photocatalytic performance for oxygen evolution (about a 2-fold increase compared with that of the pristine ZnCr-LDH).[171] Tb provided a prompt conduction of the photo-induced electrons and the injection of electrons of Tb accelerated the target reactions. In another example, Mikami *et al*. found that anchoring gold nanoparticles on ZnAl-LDH could remarkably enhance photocatalytic degradation of phenol under solar light irradiation.[126] The specific charge transfer between the gold nanoparticles and the ZnAl-LDH and the surface plasmon resonance of gold particles contributed significantly to the enhanced photocatalytic response (Figure 5c).

Table 4. Representative LDH-based hybrids anchored with semiconductors in recent years.

| LDH | Anchoring materials | | Performance vs. the pristine LDH | Ref. |
|---|---|---|---|---|
| | Material | type | | |
| MgAl | CdS | Semiconductor | Much superior catalytic activity for $H_2$ generation than that of CdS (up to 20 times) | 17 |
| MgFe | Molybdate | Semiconductor | Enhanced photocatalytic activity for organic contaminant | 161 |
| ZnAl | g-$C_3N_4$/CuO | Semiconductor | Enhanced photodegradation activity toward phenol | 162 |
| ZnAl | ZnS | Semiconductor | Exhibited a large enhancement of the photocatalytic degradation activity for organic dyes | 163 |
| ZnAl | $TiO_2$ | Semiconductor | Improved overall photocatalytic performance; enhanced antibacterial performances in water purification processes | 164, 165 |
| ZnFe | $TiO_2$ | Semiconductor | Largely promoted performances in the photoelectrochemical water splitting | 160 |
| ZnCr | CdSe | Semiconductor | Remarkably suppressed the photogenerated electron-hole recombination; significantly enhanced photocatalytic activity for $H_2$ generation | 125 |
| NiFe | $TiO_2$ and reduced graphite oxide | Conductive Material and semiconductor | Simultaneously enhanced the charge separation and water oxidation efficiency | 23 |
| NiFe | g-$C_3N_4$ and N-doped graphene | Conductive Material and semiconductor | Enhanced solar-driven photoelectrochemical water oxidation | 166 |
| NiFe | g-$C_3N_4$ | Semiconductor | Enhanced photocatalytic activity towards water oxidation and reduction reaction | 167 |
| NiFe | BiOCl | Semiconductor | Enhanced photo-degradation of dye | 168 |
| NiFe | $NiCo_2O_4$ | Semiconductor | Highly efficient overall water-splitting activity | 169 |
| NiCo | $MoS_2$ | Semiconductor | Exhibited an extremely low hydrogen evolution reaction overpotential of 78 mV at 10 mA/cm$^2$ and a low Tafel slope of 76.6 mV/dec in 1 M KOH solution; more stable | 159 |
| CoNi | BiOBr | Semiconductor | Showed much higher adsorption and photocatalytic properties for organic dyes and phenol under UV-light irradiation | 16 |
| CoAl | CdTe and $BiVO_4$ | Semiconductor | Highly enhanced photoelectrochemical water oxidation efficiency | 124 |
| CoAl | $TiO_2$ | Semiconductor | Enhanced photocatalytic reduction of $CO_2$: exhibited good activity and selectivity (>90%) for aqueous $CO_2$ photoreduction to CO, without a sacrificial hole acceptor | 170 |

Table 5. Representative LDH-based hybrids anchored with rare earth elements and noble metals.

| LDH | Anchoring materials | | Performance vs. pristine LDH | Ref. |
|---|---|---|---|---|
| | material | type | | |
| ZnSn | $CeO_2$ | Semiconductor and Rare earth element | Enhanced photocatalytic performance for phenol photodegradation under UV light | 173 |
| MgAl | $CeO_2$ | Semiconductor and Rare earth element | Enhanced photocatalytic activity for $H_2$ production | 174 |
| MgAl | Tb | Rare earth element | Exhibited strong green emission response to L-lysine (L-lysine sensor) | 175 |
| MgAl | Pd | Noble metal | Excellent catalyst for selective synthesis of primary anilines from cyclohexanone oximes with high yields | 176 |
| MgAl | Ru | Noble metal | Displayed significant catalytic activity for selective $CO_2$ hydrogenation to produce formic acid | 172 |
| MgAl | Pt | Noble metal | Effective and stable catalyst for glycerol steam reforming | 177 |
| MgAl and MgAlCe | Au | Noble metal | Highly efficient reductive degradation of organic contaminants | 178 |
| MgZnAl | Au-Pd | Noble metal | Enhanced photocatalytic degradation of organic dye | 179 |
| MgCaAl | AuPd and La | Rare earth element and noble metal | Highly efficient bimetallic catalysts with the enhanced stability for a wide range of base-free aerobic oxidation of organic contaminants in water | 180 |
| ZnAl | Ce | Rare earth element | Enhanced phenol catalytic decomposition: $Ce^{4+}$ acted as electron scavenger, facilitating the electron transfer toward adsorbed $O_2$ and an accumulation of holes, increasing the generation of radicals OH· | 181 |
| ZnAl | Au | Noble metal | Enhanced phenol catalytic decomposition under solar light | 126 |
| ZnCr | Tb | Rare earth element | Largely enhanced visible light photocatalytic performance: effective separation of photo-induced charge carriers and high charge injection efficiency | 171 |
| ZnTi | Ag | Noble metal | Much higher photocatalytic activity and photochemical stability | 182 |
| ZnGa | Ag or Au | Noble metal | Much higher photocatalytic activity and selectivity for conversion of carbon dioxide | 183 |
| CoAl | Ag | Noble metal | Highly sensitive flexible piezoresistive materials | 184 |

### 2.4 Regulation of layer composition

The LDH structure type is very accommodating to changing the metal components, their molar ratios, and oxidation states. The ionic radii of the two metal cations is the principal guiding concept to assess the feasibility of a particular metal cation combination for the hydroxide layers .[185] As a result the physical properties of an LDHs can be greatly controlled by this very flexible chemical composition space.[186]

#### 2.4.1 Regulation of metal components

The flexible LDH structural platform offers an effective means to adjust the chemical, coordination, and oxidation states within an LDH. Adding and reducing metal component(s), or replacing the metal component(s) with different metal(s) regulates the properties of LDHs.[26, 114, 187-189] For example, Parida *et al*. prepared MgAlFe-LDH by the incorporation of $Fe^{3+}$ into MgAl-LDH framework with the aim of investigating the role of iron in photocatalytic activity for $H_2$ generation.[189] The sample with the highest concentration of iron in the LDH layer was found to be the most effective catalyst towards hydrogen evolution under visible light irradiation. Wang and coworkers also found that the incorporation of iron could enhance the electrochemical performance of LDHs for oxygen evolution reaction.[114] In another example, Liu *et al*. demonstrated that the electrocatalytic activity of NiFe-LDHs for oxygen evolution reaction in alkaline conditions could be notably increased by aluminum substitution, because the introduction of trivalent Al ions could adjust the ratio of low-coordinated Ni and Fe atoms.[26] Furthermore, the number of active sites (defects) could also be greatly increased by the partial etching of Al species in strong alkaline solution, which further increased the activity toward oxygen evolution reaction.[26] However, when investigating the performance of NiAlCo-LDH in rechargeable NiZn battery, Gong and coworkers found that the existence of the element Co could slightly inhibit the performance (e.g., capacity) of NiAlCo-LDH compared to that of NiAl-LDH.[25] This is probably because $Co^{2+}$ can suppress the oxidation of $Ni^{2+}$ to a higher oxidation state. Therefore, the addition of new metal components may also present suppression in improving performances of LDHs; in other word, the reduction of some pre-existing metal elements in certain LDHs may also improve the properties of LDHs. The above examples demonstrate that the incorporation of new metal component(s) into LDH framework and reduction of metal component(s) from LDH can alter various properties of LDHs.

By replacing the metal component(s) with different metal element(s) of LDH, the properties of LDHs can also be tuned. In one instance, Li *et al*. prepared NiAl, CoAl, MnAl, NiCo, NiMn, and CoMn-LDH to investigate the synergistic effect between different metal components on the electrochemical behaviors of LDHs.[188] It was demonstrated that the LDHs with dual transition metals possessed lower band-gap energies and higher conductivities than mono-transition metal-based samples. The reduced band-gap energy and enhanced conductivity should be ascribed to the hybridization between 3d-orbitals of different transition metal atoms. As a result, the LDHs with dual transition metals exhibited lower charge transfer resistances and redox potentials as well as longer electron lifetime, thus they could be oxidized or reduced

more easily during the redox process. According to their results, NiMn-LDH possessed the lowest charge transfer resistance and longest electron lifetime, which signified that the synergistic effect between $Ni^{2+}$ and $Mn^{4+}$ was the best.

Table 6 presents representative examples of altering properties of LDHs by the regulation of metal component(s). As one can observe, on one hand, the regulation of metal component(s) can significantly improve various performances of LDHs, which can be ascribed to several reasons, including endowing LDHs with the specific characteristic of a certain metal ion, modifying surface structure and crystallinity, increasing specific surface area, improving electronic structure and conductivity, adjusting band-gap, and creating defects. On the other hand, tuning the metal component(s) by introducing improper metals may also inhibit the performance of LDHs.

Table 6. Representative examples of the regulation of metal components: regulation types, performance or characteristics, and reasons for the changes of properties.

| Pristine LDH | Regulation types | Performance or characteristic | Reasons for the changes of properties | Ref. |
|---|---|---|---|---|
| MgAl | Addition of $Fe^{2+}$ in layers | Endowed the LDH with the ability to reduce hexavalent chromium | The reducing activity of $Fe^{2+}$ | 190 |
| MgAl | Addition of $Fe^{3+}$ in layers | Enhanced hydrogen evolution activity under visible light irradiation | The enhanced performance was attributed to the favorable surface structure and higher crystalline nature of hydrotalcites | 189 |
| (Mg or Zn)Al | Metal composition replacement (between Mg and Zn) | MgAl-LDH possessed a much higher electric conductivity than that of ZnAl-LDH | The difference in electric conductivity is due to the differing ionic radii and electronic structures of the intralayer metal cations, as well as the different degrees of distortion of the $MO_6$ octahedron in the 2D LDH layers. | 75 |
| NiAl | Addition of $Co^{3+}$ in layers | Slightly inhibited the performance in NiZn battery | This could be due to Co suppressing the oxidation of $Ni^{2+}$ to a higher oxidation state | 25 |
| NiFe | Addition of $Mn^{4+}$ in layers | Superior oxygen evolution activity | The addition of $Mn^{4+}$ can modify the electronic structure and improve the conductivity of the electrocatalyst | 187 |
| NiFe | Addition of $Al^{3+}$ in layers and partial etching/dissolution of the incorporated $Al^{3+}$ | Higher activity and stability than NiFe-LDH for oxygen evolution reaction | Al substitution increased the concentration of Ni active sites on the catalyst surface. Besides, low-coordinated Ni and Fe atoms and defects were formed by partial etching/dissolution of $Al^{3+}$ in alkaline solution, further increasing the activity towards oxygen evolution reaction | 26 |
| NiCo | Addition of $Fe^{3+}$ in layers | The Fe-incorporation significantly enhanced the electrochemical performance of the material for oxygen evolution reaction | This was ascribed to the enhanced conductivity and improved intrinsic catalytic activity, a large surface area, and a high porosity structure of the material | 114 |
| NiCo, NiCoFe | Addition of $Al^{3+}$ in layers | Superior specific capacitance of 1153 $Fg^{-1}$ at 6 $Ag^{-1}$, and excellent cycling stability (ca. 92.97% capacitance retention after 3000 cycles). | The corporation of $Al^{3+}$ led to the improvement of the electrochemical performance; $Al^{3+}$ could regulate the crystallinity, hydrophilicity and nanosheets stacking of LDH | 191 |
| NiAl, CoAl, MnAl, NiCo, NiMn, CoMn | Metal composition replacement | LDH with dual transition metals possessed lower band-gap energies and higher conductivities than mono-transition metal-based samples | The reduced band-gap energy and enhanced conductivity should be ascribed to the hybridization between 3d-orbitals of different transition atoms | 188 |
| ZnCr | Addition of $La^{3+}$ in layers | Enhanced photo catalytic activity for organic contaminant degradation under visible light irradiation | The increased surface area and light harvesting ability | 192 |
| ZnAl | Addition of $Co^{2+}$ or $Cu^{2+}$ in layers | Enhanced photocatalytic activities for organic contaminants degradation | Well-crystallized structure; the homogenously dispersed Co suppressed the recombination of holes and electrons and improved charge transfer in the ZnAl-LDH framework | 193 |
| MgAl | Regulation of molar ratios | $HAsO_4^{2-}$ uptake amounts on LDH varied with Mg/Al ratio | The amount of $Al^{3+}$ affected the charge density, basal spacing, and the exchange of interlayered anions of MgAl-LDH | 194 |
| MgAl | Regulation of molar ratios | LDH with higher $Al^{3+}$ content exhibited better adsorption performance for norfloxacin both in adsorption rate and adsorption capacity | Higher charge density gave a reinforced electrostatic attraction between LDH and anionic species | 195 |
| MgAl | Regulation of molar ratios | MgAl-LDH with different Mg/Al ratios had different surface physical properties, crystallinities, and $CO_2$ adsorption capacities | The changes of surface porosity, surface area, and crystallinities | 196 |
| MgAl | Regulation of molar ratios | Antimonate uptake amounts increased as the Mg/Al molar ratio decrease from 4 to 2 | Thanks to the increasing excess of positive charge of LDH sheets and the expanding interlayer spacing | 197 |
| MgCaAl | Regulation of molar ratios | LDH with different Mg/Ca/Al ratios had different surface physical properties and adsorption capacities for fluoride and protein | - | 198 |

| | | | | |
|---|---|---|---|---|
| ZnAl | Regulation of molar ratios | The crystallinity of LDH were found to improve as Zn/Al molar ratio decreased; band gaps were affected by the variation of the Zn/Al ratio | The decreased crystallinity was attributed to the distortion of the hydroxide layer networks of the LDH crystal by the larger difference in ionic radii of $Zn^{2+}$ and $Al^{3+}$; the formation of the low crystalline phases (ZnO and $ZnAl_2O_4$) affected the band gaps | 199 |
| ZnAl | Regulation of molar ratios | Low Zn/Al molar ratios showed limited influence to the morphology and surface area; high Zn/Al molar ratios decreased the surface area | - | 200 |
| ZnTi | Regulation of molar ratios | All the ZnTi-LDH with Zn/Ti molar ratio of 2:1, 3:1 and 4:1 displayed high photocatalytic activity under visible-light irradiation with the 3:1 one being the most active | Lower band gap, hierarchical microsphere structure, as well as high specific surface; ZnTi-LDH with Zn/Ti ratio of 3:1 had the strongest absorption in the visible light region | 201 |
| NiTi | Regulation of molar ratios | The NiTi-LDH with a Ni/Ti molar ratio of 4:1 displayed the highest photocatalytic $H_2$ production activity, in comparison with a LDH with a Ni/Ti ratio of 2:1, 3:1, and 5:1 | - | 202 |
| NiFe | Regulation of molar ratios | The NiFe-LDH with different Ni/Fe molar ratio showed different electrocatalytic activities | Ni/Fe molar ratio affected the crystallinity of NiFe-LDH; too small or large amounts of Fe will not form the NiFe-LDH phase properly | 203 |
| NiCo | Regulation of molar ratios | As the content of nickel increased, the hydroxides tended to have a higher specific capacitance with a gradually deteriorative rate capability | The addition of Ni could increase the conductivity of Ni-Co binary hydroxides | 204 |
| NiMn | Regulation of molar ratios | Ni/Mn molar ratio affected the oxygen evolution reaction activity of NiMn-LDH; NiMn-LDH with a Ni/Mn ratio of 3 showed the best performance (highly active and stable) | NiMn-LDH with a Ni/Mn ratio of 3 exhibited a high degree of crystallinity, large interlayer spacing, large surface area, and highly porous structure | 205 |
| CoFe | Regulation of molar ratios | LDH with different molar ratio presented different adsorption abilities toward organic contaminants, and CoFe-LDH with a Co/Fe ratio of 4 showed the highest affinity to organic dye methyl orange | Different porous structures | 206 |
| Co($Fe^{2+}$, $Fe^{3+}$) | Regulation of molar ratios | Co/Fe molar ratio affected the capacitive properties of the CoFe-LDH | Co/Fe molar ratio had a significant influence on the phase and structure of the products | 207 |
| ZnCo | Partial oxidation of $Co^{2+}$ to $Co^{3+}$ | The oxidation of $Co^{2+}$ affected the magnetic susceptibility of ZnCo-LDH | The co-existence of high spin $Co^{2+}$ and low spin $Co^{3+}$ | 208 |
| NiCo | Partial oxidation of $Co^{2+}$ to $Co^{3+}$ | Enhanced electrochemical performance | Enhanced electron transportation | 209 |
| NiCoFe | Partial oxidation of $Co^{2+}$ to $Co^{3+}$ | Significantly enhanced both oxygen reduction reaction and oxygen evolution reaction activity | The partial conversion of $Co^{2+}$ to $Co^{3+}$ state, which stimulated the charge transfer to the catalyst surface | 210 |
| NiFe | Partial oxidation of $Ni^{2+}$ to $Ni^{3+}$ | High catalytic activity in water splitting | The generation of effective $Ni^{3+}$ sites on NiFe-LDH | 211 |
| NiTi | Partial oxidation of $Ni^{2+}$ to $Ni^{3+}$ | Significantly improved supercapacitive performance | The decrease in the conductive resistance of the materials caused by the introduction of $Ni^{3+}$; that is, $Ni^{3+}$ served as more conductive species | 27 |
| NiFe<br>NiCo<br>CoFe<br>NiCoFe | Reduction of Ni, Fe, and Co | Dramatically promoted the overall water splitting performance | The reduced metals could finely tune the surface electronic state | 212 |

### 2.4.2 Regulation of ratio of metal components

The properties of LDHs can be fine-tuned by adjusting the molar ratio of the metal components. For example, Zhao *et al*. found that the molar ratio of Ni/Ti could significantly affect the catalytic activities of NiTi-LDH.[202] The NiTi-LDH with a Ni/Ti molar ratio of 4:1 displays the highest photocatalytic activity in $H_2$ production, in comparison with the LDH with a Ni/Ti ratio of 2:1, 3:1, and 5:1. Sumboja *et al*. also revealed that the molar ratio of LDHs greatly influenced their catalytic activity.[205] In their study, they demonstrated that NiMn-LDH with the optimized Ni/Mn molar ratio (3:1) had good crystallinity, large interlayer spacing, and large surface area, all of which were beneficial to enhance their catalytic activity. Apart from the catalytic performances, regulation of the molar ratios of metal components of LDHs can also tune other properties. For instance, Zhang *et al.* found that the electrochemical performance of NiCo-LDH was closely related to the molar ratio of Ni/Co.[204] As the content of nickel was increased, the sample tended to have a higher specific capacitance. Their electrochemical data demonstrated that the binary hydroxide with a Ni/Co molar ratio of 7:3 could deliver the maximum specific capacitance of 1803.6 $Fg^{-1}$, while the binary hydroxide with a Ni/Co molar ratio of 3:7 exhibited a high rate capability. These results indicated that increasing the amount of Ni could increase the conductivity of Ni-Co binary hydroxides. On the other hand, different Ni/Co ratios would result in different basal spacing of NiCo-LDH. The experimental results also gave a clue

that the charge storage stability and rate capability of these hydroxides highly depended on the basal spacing of NiCo-LDH. A higher basal spacing corresponds to a better electrochemical performance. In another example, Kim *et al*. systematically investigated the effect of Mg/Al molar ratio (between 3 and 30) on the adsorption of $CO_2$ by MgAl-LDHs.[196] When the Mg/Al molar ratio was between 12 and 30, these MgAl-LDHs showed a unique two-step $CO_2$ adsorption behavior: low $CO_2$ loading initially followed by a gradual transition to very high $CO_2$ loading. The $CO_2$ adsorption capacity for the MgAl-LDH with an Mg/Al molar ratio of 20 exhibited the highest reported value. The different adsorption behaviors may be ascribed to the different pore structures, surface areas, and crystallinities resulted from the different Mg/Al molar ratios.[196]

Table 6 presents examples of how altering the molar ratio of metal components may alter the properties of LDHs. As shown in Table 6, by regulating the molar ratio of the metal components in LDHs, one can generally adjust the crystallinity, basal spacing, charge density, surface area, porous structure, distortion of layers, electron conductivity of layers, and/or band-gap structure of LDHs, and subsequently obtain LDHs with tunable properties.

#### 2.4.3 Regulation of chemical valence of metal components

Generally, regulating chemical valence state of the metal components of LDHs can modify the electronic structure of individual components, thus changing the properties of LDHs.[27, 209, 210, 212] In a particular instance, Gou *et al*. reported that tuning the valence state of Co in NiCo-LDH could be an effective method to significantly improve the rate performance of NiCo-LDH, which was realized through a facile in situ chemical treatment of phosphites.[209] The specific capacitance of the obtained rosette NiCo-LDH electrode was 1425 $Fg^{-1}$ at 20 $Ag^{-1}$, which was 83.9% of 1698 $Fg^{-1}$ at 1 $Ag^{-1}$. Meanwhile, a moderate cycling stability with an efficiency of 80.6% after cycling 4000 times at a current density of 10 $Ag^{-1}$ was obtained. Moreover, an energy density of 40.1 $Whkg^{-1}$ at a power density of 801.2 $Wkg^{-1}$ was achieved in an assembled aqueous asymmetric supercapacitor, using NiCo-LDH as the positive electrode material and activated carbon as the negative electrode material. Their study showed that the chemical treatment evoked morphology and phase transformation and induced partial $Co^{2+}$ conversion to a more conductive $Co^{3+}$ state. The electrochemical performance is also highly related to the valence state of Cobalt. Qian and coworkers demonstrated that tuning the valence state of a metal component of LDH could notably enhance the performance of the LDH.[210] In their research, the $Co^{2+}$ in NiCoFe-LDH was partially oxidized to $Co^{3+}$ by $H_2O_2$, which significantly enhanced both oxygen reduction reaction and oxygen evolution reaction activity of NiCoFe-LDH. This phenomenon was attributed to the partial conversion of $Co^{2+}$ to $Co^{3+}$ state in the pre-oxidation step, which stimulated the charge transfer to the catalyst surface.

Table 6 presents typical examples of the changes the chemical valence states of the metal components of LDHs. In these examples, transition metals such as Ni, Co, and Fe are the most common metals to be regulated. The change of valence state of the metal components within LDHs is commonly a key factor to enhancing catalytic activities and electrochemical performances (e.g., supercapacitor performance) of LDHs.

### 2.5 Size and morphology control

Since the decrease of particle size, thickness and the diversification of morphologies of LDHs have a significant impact on their electronic, catalytic, and adsorption properties and thus potential applications,[213-216] considerable efforts have been focused on tuning the particle size and thickness, as well as the morphology of LDHs in the past decade.[6, 213-218]

#### 2.5.1 Size refinement

Downsizing LDHs (i.e., lowering particle size or thickness of LDH layers) offers a significant opportunity to enhance a range of LDH properties that are attributed to factors such as more coordinatively unsaturated metal cations (i.e., defect-rich structures which serve as active centers), more available exposed active sites, larger specific surface area, and higher electronic conductivity than the bulk LDHs.[27, 214, 215, 219-222] For example, Zhao *et al*. found that the decrease of the size of NiTi-LDH by *in situ* preparing monolayer LDH nanosheets contributed greatly to the improvement of its supercapacitor performance.[27] It was reported that the NiTi-LDH nanosheets exhibited a maximum specific capacitance of 2310 $Fg^{-1}$ (at 1.5 $Ag^{-1}$), which is unprecedented and 6 times higher than that of the bulk counterpart (377 $Fg^{-1}$). Furthermore, it could maintain a remarkable rate capability and high durability. The NiTi-LDH nanosheets with highly exposed chemically reactive sites and a large specific surface area ensured an efficient supercapacitive reaction. Zhao *et al*. also found that the coordinatively unsaturated metal ions in ultrathin ZnAl-LDH contributed significantly to the photocatalytic activity in $CO_2$ reduction.[215] Due to the dramatic enhancement of various properties of LDHs via decreasing size or thickness, huge innovative efforts have been devoted to advance the approaches of preparation of ultrafine or ultrathin LDHs.

The methods to prepare ultrafine or ultrathin LDHs are mainly based on two pathways, i.e., bottom-up and top-down strategies.[6] The bottom-up strategy is to prepare ultrafine or ultrathin LDHs from initial metal salts, while the top-down pathway is to decrease the particle size or thickness of the pre-existing LDHs. Generally, controlling or separating the nucleation and crystallization processes of LDHs, such as using limited space under controlled reaction conditions to induce the formation of LDHs, is an effective bottom-up means to prepare ultrafine or ultrathin LDH (Figure 6A-D).[27, 223] For example, Hu and O'Hare were the first to utilize a water-in-oil reverse microemulsion as a LDH synthesis microreactors providing only limited space and nutrients for the proceeding reactions to prepare ultrafine MgAl-LDH.[224] By limiting the available space and nutrients the nucleation and crystallization processes could be very precisely controlled, and the prepared MgAl-LDH possessed uniform nanometer sizes typically with a diameter of 40-50 nm and a thickness of *ca*. 10 nm. Wang *et al*. also reported a method by using a continuous-flow hydrothermal reactor to prepare ultrafine CaAl-LDH and MgAl-LDH.[225] In this method, the nucleation and aging time can be controlled to be very short (e.g., 4 s), which prevents the growth of the LDH nanosheets. These examples indicate that the control of nucleation and crystallization (under aging state) is highly important in bottom-up strategy to prepare ultrafine LDH. Sun and coworkers developed a unique approach to prepare LDH single-layer nanosheets by growing LDH in formamide, which serves as an effective blocking agent to selectively block the growth of the LDH in the thickness direction.[217, 218] Their preparing procedures are shown in Figure 5E.

 

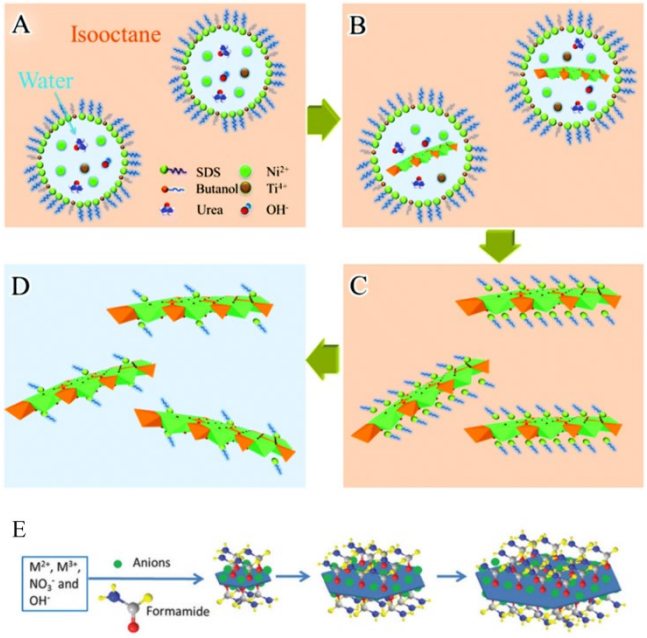


Figure 6. Schematic of the formation of monolayer NiTi-LDH nanosheets in micelles (limited space): (A) metal salts and urea mix in water droplets; (B) LDH starts to form during the hydrolysis of urea; (C) monolayer NiTi-LDH nanosheets form in isooctane; (D) monolayer NiTi-LDH nanosheets are transferred into the water surrounding after cleaning.[27] Reproduced with permission from ref.[27], Copyright 2015, The Royal Society of Chemistry; (E) direct growth of MgAl-LDH single-layer nanosheets with the assistance of layer growth inhibitors (i.e., formamide).[217] Reproduced with permission from ref.[217], Copyright 2015, The Royal Society of Chemistry

In the top-down pathway, the most prevalent and effective, but meanwhile very demanding, approach is the exfoliation of the layers into individual nanosheets. In this way, inorganic layers with a very high aspect ratio may become thoroughly separated. A summary of exfoliation methods can be found in the literature.[6, 226] After exfoliation, various properties of the LDHs usually exhibit a pronounced enhancement compared to those of the pristine LDHs.[221, 222, 227] For instance, Song and Hu demonstrated that the exfoliated CoCo-LDH, NiCo-LDH, and NiFe-LDH single-layer nanosheets exhibited significantly higher oxygen evolution activity than the corresponding bulk LDH in alkaline conditions.[221] The exfoliated nanosheets from NiFe-LDH and NiCo-LDH outperformed both the activity and stability of a commercial iridium dioxide catalyst. The improvement of the catalytic activity in oxygen evolution reaction is attributed to the more active sites created by exfoliation and the improved electronic conductivity. Sun *et al.* also confirmed that the ultrathin MgAl-LDH, CoAl-LDH, CoCo-LDH, and NiCo-LDH prepared from exfoliation could exceptionally improve the electronic and hydroxyl ion conductivities.[222] They found that the above LDH single-layer nanosheets exhibited exceptionally high in-plane hydroxyl ion conductivity approaching $10^{-1}$ S cm$^{-1}$ (the bulk LDHs generally up to $10^{-3}$ S cm$^{-1}$), which was the highest among anion conductors and comparable to proton conductivity in commercial proton exchange membranes (e.g., Nafion®). This 2D superionic transport characteristic might have great promises in a variety of applications including alkaline fuel cells and water electrolysis.

### 2.5.2 Dimensional morphology regulation

It is known that the common LDHs synthesized by the conventional methods usually exhibit a plate-like morphology (i.e., 2D morphology). Although LDHs with a 2D morphology possess fascinating functions, tuning their dimensions may endow LDHs with more attractive characteristics. In modern research, 3D hierarchical nanostructures have drawn considerable attention due to their unique properties and potential applications.[213] The fabrication of LDHs with a 3D morphology has been demonstrated to be an effective means to introduce unique performances to LDHs.[228-231] Li and coworkers developed a facile, inexpensive, and self-assembling strategy to massively fabricate a 3D rosette NiCo-LDH under mild reaction conditions (55 °C) via one-step chemical co-precipitation in metal-ammine mixture solution (Figure 7a). After systematic investigation of various reaction factors including the Ni/Co feeding ratio, reaction time, and initial pH value, the authors managed to regulate the morphologies of NiCo-LDH from nanoparticles and nanosheets to nanopetals, and eventually to rosette microspheres. The resultant 3D NiCo-LDH was demonstrated to have high electrochemical performance with an excellent capacitance value of ca. 2228 Fg$^{-1}$ (1 Ag$^{-1}$). In another instance, Li et al. prepared a rosette NiAl-LDH using a template-free and facile self-assembling hydrothermal synthesis method in the existence of poly(sodium-p-styrene-sulfonate).[230] The prepared 3D rosette NiAl-LDH exhibited excellent energy storage performance, which was much higher than that of the common NiAl-LDH. Apart from rosette 3D morphology, other 3D morphologies, such as cone-shaped[232] and vertically aligned nanosheets[228] have also been developed, and these 3D LDHs displayed high performances in various fields. The high performances of 3D LDHs can be ascribed to, but not limited to, some of the following aspects:[137, 213, 228, 229, 231] (1) 3D structures can produce a relatively high specific surface area and/or unique hierarchical porous 3D architectures; (2) the highly oriented and rigid 3D architecture can help overcome the problem of low conductivity in conventional LDHs; (3) many 3D LDHs are composed of thin LDH nanosheets; (4) 3D LDHs may have higher surface activity than common 2D LDHs.

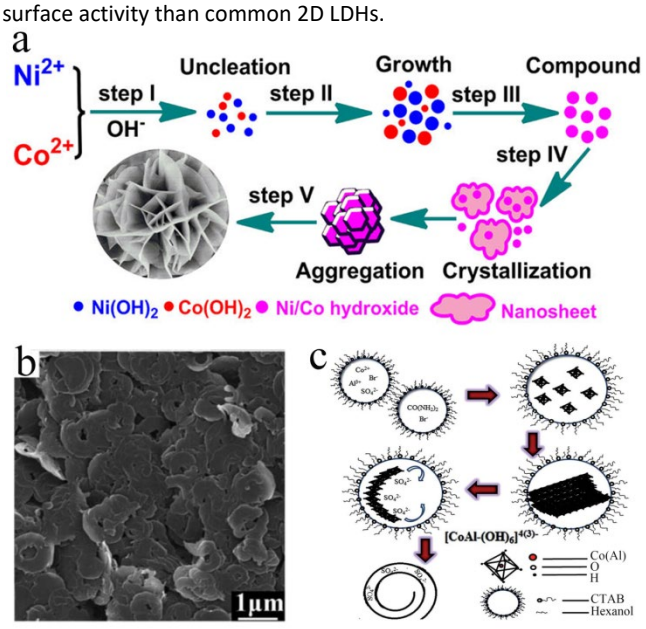


Figure 7. (a) Schematic illustration describing the synthetic procedures of the 3D NiCo-LDH microspheres,[229] Reproduced with permission from ref.[229], Copyright 2016, American Chemical Society; (b) SEM image of MgAl-LDH nanorings,[233] Reproduced with permission from ref[233], Copyright 2011, The Royal Society of Chemistry; (c) schematic of the nucleation and structural

evolution process of the CoAl-LDH nanoscrolls,[234] Reproduced with permission from ref.[234], Copyright 2015, The Royal Society of Chemistry

In addition to 3D morphologies, other morphologies such as LDH nanorings,[233] nanoscrolls,[234] nanorods,[235] and nanowires[236] have been reported, offering options to modify the characteristics of LDHs. Yang and coworkers synthesized unique MgAl-LDH nanorings with an external diameter of ca. 750 nm and an internal diameter of 250 nm in an organic/water solvent system via a urea hydrolysis method by using $Mg_{10}(OH)_{18}Cl_2{\cdot}5H_2O$ nanowires as the precursor (Figure 7b).[233] The resultant unique MgAl-LDH nanorings had a higher specific surface area and larger pore volume than the plate-like LDHs. Furthermore, the MgAl-LDH nanorings presented a significantly enhanced catalytic performance in the Knoevenagel reaction between benzaldehyde and diethyl malonate compared to the plate-like LDH. Lv *et al*. prepared a novel 1D CoAl-LDH, i.e., nanoscrolls, by facile trinal-phase hydrothermal treatment under different pressures (generated by controlling temperature).[234] Their study indicated that CoAl-LDH nanosheets formed at first, which subsequently evolved into nanoscrolls (Figure 7c). Notably, their investigation results confirmed that the urea and pressure played key roles in the formation of the 1D CoAl-LDH nanoscrolls. Further observations by scanning electron microscopy and high-resolution TEM indicated that the nanoscrolls were derived from nanosheets through a roll-up process, rather than through the control of the crystal growth in one particular direction. Owing to the increased specific surface area and novel structure, the nanoscrolls exhibited high adsorption capacity and excellent reusability in the adsorption of organic contaminant (methyl orange) in aqueous solution. These examples demonstrated that the fabrication of LDHs with special 2D (e.g., nanorings) or 1D morphology also helps the regulation of physical properties (such as surface area and porosity) of LDHs.

### 2.5.3 Hollow and porous structures

Recently, much attention has been paid to nanostructured materials with a hierarchical architecture due to their large specific surface area, high porosity, high structural stability, as well as significantly enhanced performances, e.g., electro-chemical responses, high ionic transport, enhanced adsorption capacity and catalytic activity, in comparison with their common counterparts.[237, 238] LDH is one type of such widely studied nanostructured materials. Fabrication of hierarchical LDHs with a hollow or highly porous structure is currently an active approach to control the properties of LDHs. Various researchers have found that hollow or porous LDHs can be prepared by using a template,[237, 239-242] applying bubbles,[243] or employing acid or alkali to etch LDHs.[244] For example, Shao and coworkers synthesized hierarchical MgFe-LDH microspheres with a tunable interior structure via a facile and cost-effective method by using sodium dodecyl sulfonate (SDS) as the template.[237] By controlling the concentration of SDS, the structure of the products could be tailored from hierarchical rosette MgFe-LDH solid spheres to yolk-shell and then to hollow spheres with different interior space (Figure 8a). The changes in interior space eventually contributed to the changes in specific surface area and pore-size distribution. Specifically, the maximum specific surface area of the hollow MgFe-LDH microspheres (213.6 $m^2/g$) was much larger than that of the yolk-shell (124.4 $m^2/g$) and solid (78.8 $m^2/g$) one. In addition, the pore size analysis based on the isotherms indicated that these samples consisting of a mesoporous distribution in the range of 2-6 nm. Their subsequent application results indicated that the hollow MgFe-LDH microspheres exhibited to be most promising in electrocatalytic oxidation of ethanol in alkaline fuel cells, including high activity, enhanced long-term durability and cycling stability. The high performance of the hollow LDH is a result of significantly improved faradaic redox reaction and mass transport contributed by the high specific surface area and hollow and mesoporous structures. In another instance, Rodriguez et al. developed a bubble method to prepare porous MgAl-LDH by the intercalation and decomposition of hydrogen peroxide, in which oxygen nano-bubbles were generated and subsequently pierced holes in the galleries of LDH (Figure 8b).[243] The decomposition of the peroxide can be triggered by microwave radiation or chemically by reaction with iodide ($I^-$) ions. The presence of hydrogen peroxide in the interlayer space and its later decomposition triggered by microwave radiation generated pores in between LDH layers, increasing the specific surface area from 9 $m^2/g$ to a maximum value of 67 $m^2/g$. Different from the above strategies, Abushrenta and coworkers prepared a porous LDH by applying alkali to etch the pre-synthesized CoAl-LDH which grew on $Co(OH)_2$ plates (Figure 8c).[244] The porous structure of the CoAl-LDH significantly favored the ionic diffusion and charge transport, and provided a large contact area owing to its porous structure, leading to a high supercapacitor performance. Clearly, various approaches can be employed to prepare hollow and porous LDHs, and the fabrication of hollow and porous LDHs can usually dramatically improve various properties of LDH thanks to the unique hollow and porous structures, and high specific surface area.

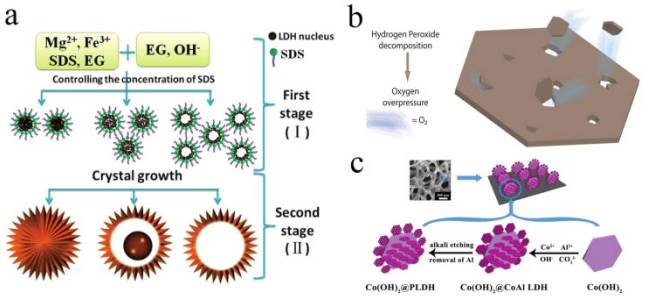


Figure 8. (a) Schematic of the morphological evolution processes of the as-obtained hierarchical rosette MgFe-LDH microspheres: (I) formation of LDH precursor-SDS micelles; (II) formation of rosette microspheres with different inner architectures,[237] Reproduced with permission from ref.[237], Copyright 2013, WILEY-VCH Verlag GmbH & Co. KGaA, Weinheim; (b) schematic of the micropore formation process in Mg-Al LDH by using the bubble method,[243] Reproduced with permission from ref.[243], Copyright 2017, Springer Nature; (c) schematic of the fabrication process of hierarchical porous CoAl-LDH arrays on $Co(OH)_2$ by alkali etching of Al,[244] Reproduced with permission from ref.[244], Copyright 2015, Springer Nature

### 2.6 Defect creation

While defects are usually highly undesirable in most materials, researchers have sought to intentionally introduce defect sites into traditional LDHs as a means of activating LDHs. For example, it was reported that defect sites (e.g., oxygen vacancies) could decrease the barrier for the adsorption of reactants, and the surface defects would lead to the formation of coordinatively unsaturated metal centers which can serve as active sites and subsequently improve electronic conductivity.[245] Previous reports also showed that, in the applications of catalysis and photocatalysis, abundant atomic defects in monolayer semiconductors could notably increase the mobility of surface

 

electrons and thus significantly enhance catalytic performance.[27] The formation of defects can usually increase the density of states near the Fermi level, which serve as active centers for catalysis.[246] In addition, defects can also create new active sites for the adsorption of reactants and increase light absorption through narrowing of the bandgap, synergistically enhancing photocatalytic activity. Therefore, defects can tune the adsorption ability, electronic conductivity, and light absorption performance of LDHs, and create more active sites for LDHs.

The above merits of defects markedly advance the diverse performance of LDHs. For instance, to improve the efficiency of visible-light-driven photocatalytic dinitrogen fixation, Zhao *et al*. designed an ultrathin CuCr-LDH with a severely distorted structure.[219] The study showed that the ultrathin CuCr-LDH photocatalyst possessed a remarkable photocatalytic activity for the photoreduction of $N_2$ to $NH_3$ in water at 25 °C under visible-light irradiation. It was demonstrated that the CuCr-LDH nanosheets contained abundant oxygen vacancies that enhanced the adsorption and activation of $N_2$ and $H_2O$, endowing the LDH nanosheets with an excellent photocatalytic activity for transforming $N_2$ to $NH_3$. It was also revealed that the introduction of $Cu^{2+}$ ions in the LDH nanosheets imparted additional structural distortions and compressive strain, leading to an increased interaction between the LDH and $N_2$, thereby promoting $NH_3$ evolution. In another work, they introduced abundant oxygen defects onto ZnAl-LDH nanosheets by controlling the particle size of the nanosheets, and demonstrated that the created abundant oxygen vacancies on the ultrathin ZnAl-LDH nanosheets could serve as trapping sites for efficient adsorption of $CO_2$ and $H_2O$ molecules, promoting the photo-induced charge separation and significantly improving the catalytic activity for $CO_2$ reduction.[215] In a report by Liu and coworkers, the defect-rich ultrathin CoFe-LDH nanosheets were proved to be highly effective in overall water splitting.[245] The defects played a key role in the improvement of water splitting performance. Therefore, creation of defects is a theoretically and practically viable and promising approach to functionalize LDHs.

## 3. Applications

LDHs have found widespread application in the past few decades. After appropriate modification or functionalization LDHs can exhibit new and/or improved function, as briefly discussed in the above section. In the following section, we will discuss a designed functionalization may be performed to achieve a specific property enhancement. For example, because of their unique physiochemical properties, functionalized LDHs are particularly suitable for environmental, energy, catalysis, and biomaterial related applications.

### 3.1 Environmental applications

With rapidly growing industrial development worldwide, the need for a new class of functional materials and techniques for treating various contaminants (e.g., heavy metals, radionuclides, and organic contaminants) remains a major concern to protect the environment. LDHs and particularly functionalized LDHs are emerging as promising materials for environmental remediation,[9, 247] especially in water systems.[9, 247, 248] Functionalized LDHs can not only provide physical but also chemical means to remove contaminants, which makes them far superior to other common materials such as activated carbons and silicates in environmental remediation. Functionalized LDHs can be used as both an adsorbent and a catalyst, which greatly exploit the physical and chemical properties of functionalized LDHs. When functionalized LDHs are used as an adsorbent, various features of the LDH (e.g., anion exchange ion or basic sites) provide active sites for many adsorbates. The facile manipulation of the adsorption sites (e.g., layer charge density, basic strength and density) by the aforementioned strategies as well as the morphology/pore structure at micron-nano scale offer a possibility to tune the active structure and adsorption kinetics for a specific adsorption process.[9] Utilizing LDHs as a catalyst, various aspects of LDHs can be regulated to achieve a high catalytic activity for the degradation of contaminants, including the flexible tunability of the metal cations in the layers, the overall morphology and pore structure, the exchangeability of the intercalated anions in the interlayer space, the accessibility of the guest functional species after hybridization (such as conductive materials, semiconductors, and noble metals or rare earth elements), and the providential defect sites.[9, 248] Herein, we will manly focus on the applications in the removal of heavy metal ions, radionuclide, and organic contaminants by functionalized LDHs.

#### 3.1.1 Heavy metals removal

The presence of heavy metal ions (e.g., $Cu^{2+}$, $Co^{2+}$, $Cd^{2+}$, $Ni^{2+}$, $Zn^{2+}$, $Pb^{2+}$, $As^{3+/5+}$, $Cr^{3+/6+}$, and $Hg^{2+}$) in our environment has raised worldwide health concerns. Heavy metals originate from wastewater and steams from a range of industries such as plastics, battery manufacturing, mining, paper, electroplating, fertilizer, and steel.[247, 249] Many heavy metal-containing complexes bioaccumulate in living organisms thus ultimately causing a serious threat to human health.[247] Therefore, the removal of heavy metals from environmental medium such as water remains a key subject of research. Previous studies suggested that functionalized LDHs exhibit very favorable adsorption to heavy metals as measured by high adsorption capacity and selectivity,[2, 66, 76, 247, 250-252] which resulted in effective removal of toxic metals to meet increasingly strict environmental regulations. For example, Ma and coworkers found that the intercalation of $MoS_4^{2-}$ into MgAl-LDH interlayer space could not only endow MgAl-LDH with the ability to adsorb various heavy metal ions ($Co^{2+}$, $Ni^{2+}$, $Zn^{2+}$, $Cd^{2+}$, $Pb^{2+}$, $Cu^{2+}$, $Hg^{2+}$, and $Ag^{+}$) rapidly and effectively, but also offer high selectivity for some of these heavy metals.[2, 66] The intercalation of $MoS_4^{2-}$ produces a 5-8 folds increase of the heavy metal cations capture capacity of the MgAl-LDH compared to that of the non-functionalized MgAl-LDH. Recently, Asiabi and coworkers have indicated that the intercalation of functional species into the interlayer space of LDH could endow LDH with a highly selectivity and efficient removal of heavy metals, and the properties (e.g., functional groups) of the intercalants played a key role in the adsorption process.[76, 251]

Apart from the functionalized LDHs produced by intercalation, various other types of functionalized LDHs were also showed to be highly effective in heavy metal removal, such as the LDH hybridized with carbon materials,[253-255] 3D LDHs,[213, 255] core-shell LDHs,[256] and ultrathin LDHs.[257] The main factors contributing to the favorable adsorption of heavy metals by the functionalized LDHs include high specific surface area and porosity, unique nanostructure, and the specific functions of the guest species hybridized with LDH.[2, 66, 213, 250, 254, 255]

#### 3.1.2 Radionuclide capture

Nuclear energy generation is considered to be an important component of an economical and sustainable energy generation strategy. However, the development of improved nuclear energy generation approaches involves developing effective management protocols for the radioactive waste at each part nuclear fuel cycle.[258] Radioactive nuclides are some of the dangerous contaminants in the environment because of their long half-life, high radioactivity, and biological toxicity.[258] In recent years, functionalized LDHs have been demonstrated to be potential candidates to remove or immobilize radioactive contaminants (e.g., U(VI), $^{129}I$, $^{99}Tc$, and $^{79}Se$) from environmental media.[3, 66, 259-267]

Functionalized LDHs can remove or immobilize radioactive contaminants mainly through surface adsorption and/or interlayer anion exchange.[267] Surface adsorption involves the attachment of a nuclide onto the surfaces of the LDHs or onto the sites of the guest species used to functionalize LDHs, forming a stable molecular or atomic film on the top of the LDH material or an aggregation on the guest species zones. In the surface adsorption process, the adsorption of radionuclide can be induced by the nature of the LDH or the guest species on LDH. The interlayer anion-exchange process involves the exchange of interlayer anions with the targeted nuclide anions and is mainly influenced by the nature of the charge balancing anions in the interlayer space, the layer charge density, and the interlayer distance.[3, 267] Ma and coworkers demonstrated that the intercalation of polysulfide into the galleries of MgAl-LDH provided MgAl-LDH a merit of highly selective and efficient capture of radionuclide ($UO_2^{2+}$).[3] The polysulfide functionalized LDH showed a high removal capacity ($q_m$ = 330 mg/g), large adsorption coeffcient values ($10^4$-$10^6$ mL/g at 1-300 ppm U concentration), and high removal rates (>95% at 1-100 ppm, or ~80% for ppb level seawater) for $UO_2^{2+}$. Their results indicated that under low U concentrations, the functional unit $(S_4)^{2-}$ coordinated to $UO_2^{2+}$ forming anionic complexes that were retained in the LDH interlayer space, while at high U concentrations, $(S_4)^{2-}$ binds to $UO_2^{2+}$ to generate neutral $UO_2S_4$ salts outside the interlayer space. In this example, the immobilization of U on LDH mainly exploits the specific functions of polysulfide. In a further study, Ma and coworkers, intercalated $MoS_4^{2-}$ in MgAl-LDH and used it to remove $^{79}Se$ ($SeO_4^{2-}$, and $SeO_3^{2-}$/$HSeO_3^-$). The removal of $^{79}Se$ preceeded by an interlayer anion-exchange process.[66] Importantly, the $MoS_4^{2-}$ intercalated MgAl-LDH presented a super high adsorption capacity for $SeO_3^{2-}$/$HSeO_3^-$ reaching 294 mg/g. This adsorption capacity for $SeO_3^{2-}$/$HSeO_3^-$ reached a record value, placing the $MoS_4^{2-}$ intercalated MgAl-LDH amongst the highest-capacity selenite adsorbing materials reported to date. Many other types of functionalized LDHs exhibit impressive performance in the capture of radionuclides, such as core-shell-type LDHs,[259] 3D LDHs,[260] LDHs hybridized with carbon or carbon related materials.[262, 265]

### 3.1.3 Water-soluble organic contaminant removal

During recent years, functionalized LDHs are increasingly investigated for the remediation of various toxic organic contaminants from wastewater due to their high surface area, outstanding anion-exchange capability, tunability and low toxicity.[247] Their high surface area and outstanding anion-exchange capacity (AEC, e.g., 272.9 mmol/100g of AEC for $Mg_4$Al-LDH[56]) make them promising candidates as adsorbents for organic contaminants such as various dyes.[247] The ease in tuning the components including layered metal compositions and the guest species, e.g., semiconductors, noble metals and rare metal elements, hybridized on LDH enables LDHs to be excellent catalysts to degrade organic contaminants.[9, 10] As such, functionalized LDHs remove organic contaminants mainly via adsorption or catalytic degradation. For example, Zhang *et al*. functionalized MgAl-LDH by hybridizing surface passivated carbon dots containing abundant oxygen-containing functional groups (-OH, -COOH, and -C=O) onto the surface of the LDH.[268] Taking advantage of the combined benefits of the LDH and the carbon dots, the as-prepared hybrids exhibited high uptake of anionic dye methyl blue (185 mg/g). The authors proposed that the cooperative contributions of hydrogen bonding between methyl blue and carbon dots, as well as the electrostatic attraction between methyl blue and LDH led to the high performance for dye removal (Figure 9a). The high adsorption performance of functionalized LDHs as adsorbents for organic contaminants has also been well demonstrated by many other researches.[247, 269-271]

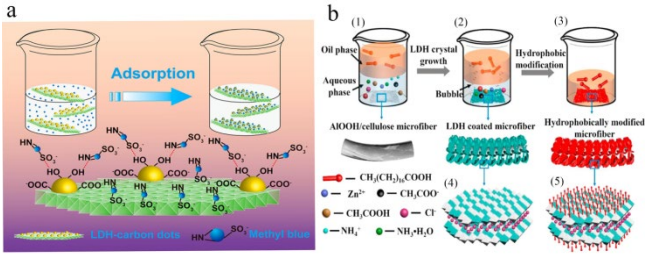


Figure 9. (a) Schematic of methyl blue adsorption onto LDH-carbon dot hybrids,[268] Reproduced with permission from ref.[268], Copyright 2014, American Chemical Society; (b) schematic of the preparation of superhydrophobic cellulose/ZnAl-LDH membrane in an open oil/water two-phase system,[272] Reproduced with permission from ref.[272], Copyright 2017, Elsevier

Besides their high performance in adsorption, various functionalized LDHs possess the ability to remove organic contaminants by catalytic degradation. The LDHs containing transition metals are semiconductors with the potential for photocatalytic environmental catalysts. Furthermore, specific guest species hybridized on LDH further improve catalytic performance in the degradation of organic contaminants. For example, Zhu and coworkers synthesized a semiconducting ZnTi-LDH, and subsequently functionalized it by surface hybridization with $C_{60}$.[8] Taking the advantages of the hybridization in promoting the electron-hole separation efficiency and enhancing the visible-light response, the functionalized LDH exhibited a significantly higher efficiency for the photocatalytic degradation of organic dyes compared the pristine LDH in the. Other types of functionalized LDHs, such as semiconductors hybridized LDHs,[273] intercalated LDHs,[274] and noble metal and rare earth element hybridized LDHs,[178] have also been reported to exhibited high performance in the degradation of organic contaminants.

### 3.14 Oil pollution elimination

The removal of oil pollutants from water is frequently required either due to oil spill accidents, or from industrial wastewater. To achieve oil removal from water, superhydrophobic and superoleophilic materials are commonly adopted.[275-280] Functionalized LDHs have been shown to offer novel opportunities as adsorbents for oil pollution remediation.[272, 281, 282] An LDH surface is inherently hydrophilic due to the abundant surface hydroxyl groups. However, the surface of LDHs can be easily modified using a wide scope of functionalization strategies as

discussed in Section **2**. For example, the incorporation of specific organic species on an LDH surface can endow LDHs with hydrophobic properties.[281] For example, Yue and coworkers developed a simple and effective strategy to fabricate a superhydrophobic cellulose/ZnAl-LDH membrane in an open oil/water two-phase system, which perfectly integrated the processes of hydrothermal reaction and hydrophobic modification (Figure 9b).[272] In this reaction system, the two dominant factors to achieve superhydrophobicity, i.e., surface roughness and low surface energy, could be accomplished simultaneously by taking advantage of crystal growth in the aqueous phase and hydrophobic modification in the oil phase. Such membranes exhibited effective separation of multiple types of oil/water mixtures, as well as excellent recyclability and exhibiting stable superhydrophobicity under harsh conditions, making them promising candidates for oily water remediation. Deploying organic surface modifiers to surface-modify LDHs for oil pollution purification has been demonstrated to be a practicable and promising approach.[281, 282]

### 3.2 Energy related applications

New energy storage and conversion technologies including hydrogen storage, supercapacitors, batteries, and solar cells have attracted tremendous attention over few decades because of the ever-increasing demand for clean and sustainable energy systems.[1, 14, 283-285] Hydrogen is a clean, efficient and renewable energy carrier; it has a high energy density and is environmentally friendly, so it is an ideal alternative to fossil fuels.[14] Water splitting by electrochemical or photochemical procedures is an environmentally benign and economic route to generate $H_2$ on a large scale. Currently, considerable efforts are being devoted to fabricating robust catalysts and storage media for $H_2$ production and storage, respectively. With respect to other energy storage systems, supercapacitors which are also referred to as electrochemical capacitors, store energy using either ion adsorption (electrochemical double layer capacitors) or fast surface redox reactions (pseudo-capacitors), enabling a rapid charge/discharge process but storing a limited amount of energy. In contrast, batteries release energy via electrochemical reactions in which ions diffuse between electrodes upon discharging. Diffusion is a slow process, but the capacity for energy storage exceeds that of supercapacitors. With regards to solar cells, the energy conversion mechanism is a light-to-electricity conversion process, with the efficiency of solar energy conversion one the main current challenges. Improving the generation and storage efficiencies of $H_2$, energy density of capacitors, power density of batteries, and the quantum efficiency of solar cells are of great interest and necessity. Herein, we give a concise introduction of the contribution of functionalized LDHs in energy field.

#### 3.2.1 Hydrogen generation

Nowadays, hydrogen is widely used in chemical processing, petroleum industry, fats and oils, metals, electronics, space exploration, utilities, and glass manufacturing.[286, 287] Hydrogen has the highest energy content by weight of 33,320 Wh $kg^{-1}$, which is about 3 and 7 times more than gasoline (12,700 Wh $kg^{-1}$) and natural gas/coal (13,900 Wh $kg^{-1}$), respectively.[288] Its high energy density and environmental friendliness make it an ideal alternative to fossil fuels. The development of more efficient electrochemical or photochemical methodologies to split water into $H_2$ and $O_2$ is one of the grand challenges of modern chemistry.[289] This requires the development of highly active, low-cost electrocatalysts and photocatalysts with superior durability for both the oxygen evolution reaction (OER) and hydrogen evolution reaction (HER). As summarized in **Section 2** and Tables 1-6, various functionalized LDHs have been shown to exhibit excellent charge transfer performance and high catalytic activities for water splitting. LDHs are relatively inexpensive to prepare commercially and since the layered structure significantly favors the diffusion of water molecules and fast release of gaseous products.[14] The exploration of functionalized LDHs as catalysts for hydrogen generation has been explored.

LDHs can be employed as robust electrocatalysts for water splitting. LDHs are commonly considered as OER catalysts, i.e., LDHs are OH-acceptors and robust catalysts for oxygen generation.[290] $Co^{2+/3+}$-, $Fe^{3+}$-, and $Ni^{2+}$-based LDH materials can effectively adsorb hydroxyl species and catalyze their dissociation, are well-known as an emerging family of efficient electrocatalysts for oxygen evolution in alkaline media.[159] Unfortunately, the HER kinetics is disappointingly sluggish in basic solutions, and the HER activity in a base is usually 2 or 3 orders lower than that in an acidic solution.[159] In addition, LDHs are unstable in acidic media. To improve the HER activity of LDHs in a basic medium, functionalizing them through specific treatments such as anchoring an H-acceptor on their surface and fabrication of unique structures, has been developed. For instance, Hu and coworkers hybridized $MoS_2$, a strong H-acceptor, on the robust OER catalyst of NiCo-LDH, and demonstrated that the hybridization endowed with a dramatic enhancement of the HER kinetics in alkaline media.[159] The functionalized NiCo-LDH exhibited an extremely low HER overpotential of 78 mV at 10 mA/$cm^2$ and a low Tafel slope of 76.6 mV/dec in 1 M KOH solution. At a current density of 20 mA/$cm^2$ or even higher, the $MoS_2$/NiCo-LDH hybrid could operate without degradation for 48 hr. This work offers us new opportunities for developing high-performance catalysts in new media. Unlike the strategy of hybridizing H-acceptor onto an LDH, Yu *et al*. found that the construction of unique 3D core-shell structures could enhance the HER performance of LDHs.[14] They fabricated a 3D core-shell LDH by growing only a few-layers of NiFe-LDH on a Cu nanowire cores supported on Cu foams (Figure 10a). Remarkably, benefiting from this 3D hierarchical nano-architecture with a large surface area, fast electron transport, and open-channels for effective gas release, the resulting 3D self-standing catalyst exhibited an outstanding OER activity as well as an excellent HER performance in an alkaline medium. Using it as a bifunctional catalyst for overall water splitting, a current density of 10 mA $cm^{-2}$ was achieved at a voltage of 1.54 V, and 100 mA $cm^{-2}$ at 1.69 V with excellent durability, which is much higher than the benchmark of $IrO_2$ (+)//Pt(-) electrodes. Other strategies, such as producing numerous active exposed edges (e.g., by size refinement) and more accessible active sites, and hybridizing conductive materials to promote charge transfer also showed benefits in enhancing HER performance of LDHs.[169, 291]

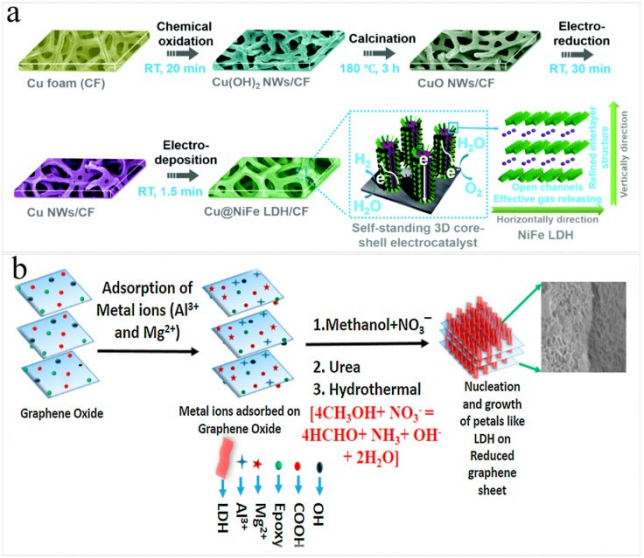


Figure 10. (a) Schematic of the fabrication procedures of the self-standing 3D core-shell Cu@NiFe-LDH electrocatalysts (RT: room temperature),[14] Reproduced with permission from ref.[14], Copyright 2017, The Royal Society of Chemistry; (b) schematic of formation of reduced graphene oxide intercalated LDH.[292] Reproduced with permission from ref.[292], Copyright 2016, Elsevier

Functionalized LDHs also exhibit very promising photocatalysis under visible light irradiation for $H_2$ generation. Wang and coworkers designed and fabricated a $Cu_2O$@ZnCr-LDH core-shell photocatalyst which delivered a high performance in visible-light driven water splitting.[98] The $Cu_2O$@ZnCr-LDH nanostructure exhibited a high activity (with $H_2$ and $O_2$ production rate of 0.90 and 0.44 μmol $h^{-1}$, respectively) under visible-light without any sacrificial agent and co-catalyst, which is among the highest level of the reported photocatalysts under the same conditions. Both experimental and computational investigations demonstrated that the $Cu_2O$@ZnCr-LDH heterostructure fully exploited the synergistic effect of $Cu_2O$ and ZnCr-LDH in terms of band structure matching. More examples of functionalized LDHs as photocatalysts for $H_2$ generation can be found in Tables 1-6.

### 3.2.2 Supercapacitors

Supercapacitors are an important class of electrochemical energy storage device, they possess the characteristics of high power density, fast charge/discharge rate, excellent cycling life, low cost, and safe operational conditions.[293-296] However, they present a low energy density, limiting the optimal discharge time to less than a minute, whereas many applications clearly require more.[293, 297, 298] Therefore, one of the challenges posed for supercapacitors is to increase energy density without compromising power density, or, alternatively, to achieve a proper balance between the two. A notable improvement in the performance of supercapacitors has been achieved through advances in the understanding of charge storage mechanisms (such as the ion behavior in small pores) and the development of advanced materials.[293] According to the surface charge-storage mechanism, two key factors; surface area and electrical conductivity, affect the performance of electrode materials in a supercapacitor.[293, 299] Given that, numerous efforts have been devoted to exploring advanced electrode materials. Functionalized LDHs have demonstrated to be effective electrode materials in supercapacitor applications owing to their unique structural and electrochemical properties.[80, 95, 99, 106, 111, 113, 292, 300]

As a typical example, Hatui and coworkers functionalized MgAl-LDH by hybridizing it with reduced graphene oxide (RGO) (Figure 10b), and the hybridization endowed the resultant material (named as RGO-MgAl-LDH) with prominent supercapacitor performances, achieving a specific capacitance up to 1334 $Fg^{-1}$ at a current density of 1 $Ag^{-1}$ in a three-electrode cell set up under 1 M aqueous KOH, and 1092.5 $Fg^{-1}$ at a current density of 2 $Ag^{-1}$ in a two-electrode configuration with 1 M tetraethyl-ammonium tetrafluoroborate ($TEABF_4$) as electrolyte.[292] RGO-MgAl-LDH also exhibited a high cyclic stability at a steady current density of 5 $Ag^{-1}$ in a two electrode organic electrolyte system with 87% retention of specific capacitance after 10000 consecutive charge-discharge cycles. This RGO functionalized LDH demonstrated both high energy and power density, at 388.26 $WhKg^{-1}$ (at a current density of 2 $Ag^{-1}$) and 3198.48 $WKg^{-1}$ respectively, in a two-electrode organic electrolyte configuration. The high performance of RGO-MgAl-LDH in the supercapacitor is ascribed to the large increase in surface area (from 288.3 for the neat LDH to 714.5 $m^2/g$ for RGO-MgAl-LDH), as well as to its unique sandwich-like structure. Such a large enhancement of the surface area allows facile electrolyte accessibility at the interior of the hybrid and significantly shortens ionic transport pathways, facilitating and delivering high capacitance as a result. Concurrently, the sandwich-like structure restricts the restacking of graphene nanosheets and hence improves the accessibility of electrolyte into the interior of the hybrid, making it a more effective electrode material. Yang *et al.* functionalized NiCoAl-LDH by coupling with NiCo-carbonate hydroxide (NiCo-CH) nanowires, and applied this nanohybrid as the positive electrode for an asymmetric supercapacitor.[300] The supercapacitor possesses a high energy density of 58.9 $Wh{\cdot}kg^{-1}$ at a power density of 0.4 $kW{\cdot}kg^{-1}$, which is based on the total mass of the active materials at a voltage of 1.6 V. An energy density of 14.9 $Wh{\cdot}kg^{-1}$ can be retained even at a high power density of 51.5 $kW{\cdot}kg^{-1}$. These results are much better than many other common supercapacitors as shown by the authors. Furthermore, the supercapacitor also exhibits an excellent long cycle life, whereby a specific capacitance of 97% is retained even after 10,000 cycles. The high performance is ascribed to the fact that the nanowire-like NiCo-CH species in the NiCoAl-LDH nanoplate matrix function as a scaffold and support the dispersion of the NiCoAl-LDH nanoplates, resulting in a relatively loose and open structure within the electrode matrix (Figure 11). Various other types of functionalized LDHs, such as intercalated LDH, core-shell structured LDH, and hybridized LDH, also present notable supercapacitor performances with a high specific capacity, stability, and energy and power density, as evidenced by the many examples summarized in Tables 1-6.

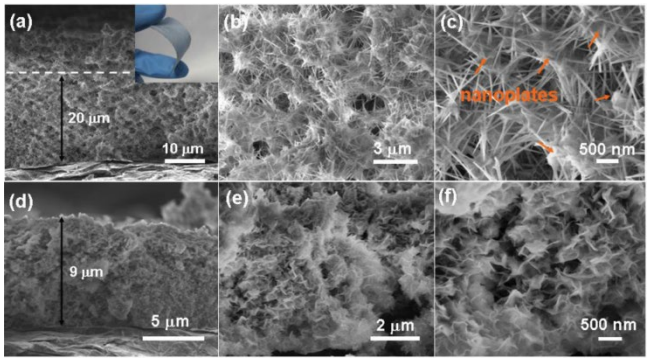


Figure 11. Representative FE-SEM images of the nanohybrids of NiCoAl-LDH and NiCo-CH grown at different $Co^{2+}$ concentrations: a–c) cross-section

of the as-obtained sample with a Co/Ni molar ratio of 1:1; d–f) cross-section of the as-obtained sample with a Co/Ni molar ratio of 1:3. Reproduced with permission from ref.[300], Copyright 2014, WILEY-VCH Verlag GmbH & Co. KGaA, Weinheim

### 3.2.3 Batteries

Rechargeable batteries, an important class of energy storage device which includes the Li-ion batteries (LIBs), Li-S batteries, metal-oxygen/air batteries, have drawn particular attention.[301-303] Among these batteries, metal-oxygen/air batteries and Li-S batteries have been considered as promising candidates for the next-generation electro-chemical energy-storage technologies because of their overwhelming advantages in energy density.[304-307] For example, the theoretical energy density of Li-$O_2$ (aq) is 3582 Wh $kg^{-1}$ and for the Zn-air system, the value is still remarkably high at 1086 Wh $kg^{-1}$.[306] For metal-oxygen/air batteries, their working principle is that during discharge, oxygen is reduced to hydroxide ions. This reaction is called the oxygen reduction reaction (ORR). During charging, oxygen is formed. This reaction is called the oxygen evolution reaction (OER). Unfortunately, one of the greatest challenges for these types of batteries is the high overpotential at the oxygen/air-cathode, i.e., at the so called gas diffusion electrode, which occurs with both the ORR and the OER.[306] To reduce the overpotential for the OER and the ORR, respectively, new generation catalysts are needed. As for Li-S batteries, some valuable characteristics of sulfur, such as its high natural abundance, low cost, and nontoxicity, make Li-S batteries even more commercially competitive than the current LIBs.[308, 309] However, practical applications of the rechargeable Li-S batteries are still hindered by a multitude of issues, including low utilization of the active material, short cycle life, fast self-discharge, and poor Columbic efficiency.[307, 310, 311] The performance of rechargeable batteries is significantly affected by the properties of the electrode materials. Thus, screening for novel electrode materials with novel structures and surface properties and the optimization of high-performance materials are areas of immense significance to the improvement of rechargeable battery performance.

Functionalized LDHs are potential candidates to the fabrication of metal-oxygen/air batteries[304-306] and Li-S batteries[307] with notable strengths, particularly low OER and ORR overpotential for metal-oxygen/air batteries and high stability and high utilization of the active sites for Li-S batteries. For example, Wang and coworkers have prepared a bifunctional electrocatalyst by hybridizing $Co^{2+}$, N-doped carbon nanoframes (Co, N-CNF) with NiFe-LDH, and found that the resultant material displayed a low OER overpotential of 0.312 V at 10 mA $cm^{-2}$ and an ORR half-wave potential of 0.790 V.[304] The outstanding performance of the electrocatalyst was attributed to the high electrical conductivity and excellent ORR activity, contributing from the combination of Co, N-CNF and NiFe-LDH. Owing to the excellent OER and ORR performance, the resultant material could be used to fabricate high-performance Zn-air battery which exhibited a low discharge-charge voltage gap (1.0 V at 25 mA $cm^{-2}$), long-term cycling durability (over 80 h), and superior overall performance to a counterpart battery constructed using a mixture of $IrO_2$ and Pt/C as the cathode. When hybridized with nickel foam, NiFe-LDH showed an even lower OER overpotential (ultralow as 0.21 V at 10 mA $cm^{-2}$), as indicated by Yan and coworkers.[305] A nickel foam functionalized NiFe-LDH exhibited attractive performance in Zn-oxygen battery with an outstanding stability of over 100 charge/discharge cycles. These reports suggest that rationally-designed functionalized LDHs offer opportunities as active materials for the fabrication of metal-oxygen/air batteries with advantages such as ultralow overpotential and high stability. In addition, Zhang *et al*. showed that functionalized LDHs displayed remarkable performance in Li-S batteries.[307] In their study a core-shell-type NiCo-LDH with $Co(OH)_2$ as the inner shell and NiCo-LDH as the outer shell was fabricated and used in Li-S battery. Specifically, the hollow $Co(OH)_2$@NiCo-LDH with a complex shell structure not only maximized the advantages of hollow nanostructures for encapsulating a high content of sulfur (75 wt%), but also provided sufficient self-functionalized surfaces for chemically bonding with polysulfides to suppress their outward dissolution. When evaluated as the cathode material for Li-S batteries, the $Co(OH)_2$@NiCo-LDH/sulfur cathode was able to maintain excellent cycling stability at both 0.1 and 0.5 C over 100 cycles, and delivered high-rate capacities with relatively high sulfur loading of 3 mg $cm^{-2}$. Therefore, functionalized LDHs with rationally designed components and structures also show promise in the construction of Li-S batteries with a high stability and the utilization of active sites.

In addition to metal-oxygen/air batteries and Li-S batteries, various studies[159, 312-315] also indicate that functionalized LDHs are of great potential in the construction of Zn-Ni secondary batteries.

### 3.2.4 Solar cells

Exploitation of solar energy is an essential component of the renewable energy strategy of the next generation society. There have already been fantastic developments in the cost effectiveness of electricity generation by solar photovoltaic technology. Developments in dye-sensitized solar cells (DSSCs) offer the promise of large quantum efficiency gains and low-cost compared to conventional inorganic photovoltaic devices. However, the present DSSCs still show some severe drawbacks. For example, the liquid electrolyte normally used for the preparation of DSSC devices poses several technical problems such as solvent evaporation, leakage of volatile solvent, and environmental toxicity, and the organic dyes have a relatively low heat stability and narrow absorption bands.[316, 317] To address the drawbacks of liquid electrolyte, methods have been developed such as adding functional materials into the electrolyte to obtain a quasi-solid electrolyte. LDH materials are found to be a highly effective additive for electrolytes. According to Wang *et al*., LDHs are capable of solidifying the electrolyte against leakage and increasing the solar cell efficiency.[318] After being modified, LDHs even exhibited enhanced functions. For instance, Bastianini and coworkers found that when high iodide intercalated ZnAl-LDH was added to the electrolyte it had positive effect on the power conversion efficiency of the DSSC compared to the low iodide intercalated and the pristine LDH.[316] In another example, Du *et al*. found that stearic intercalated MgAl-LDH could be used as an electrolyte additive to enhance the solar energy conversion efficiency of the fabricated DSSC by 2.17%.[319]

To address the drawbacks of the relatively low heat stability and narrow absorption bands of the organic dyes, one possible approach is to hybridize them with multi-functional and environmentally friendly inorganic materials such as LDHs, which can provide a stable chemical environment, increase heat or photostability, and improve the inherent light-harvesting ability of the organic dyes.[317] For example, Lee and coworkers intercalated a light sensitive organic dye (anthraquinone sulfonate anion) into the interlayer space of MgAl-LDH, and subsequently used the

intercalated LDH as the light sensitizer for DSSC.[317] The resultant hybrid showed a conspicuous photochromic property under irradiation, and this hybrid sensitized cell showed improved conversion efficiency up to 160% of the initial value from the anthraquinone sulfonate anion-sensitized cell.

### 3.3 Catalysis

LDH-based nanomaterials have found extensive applications in catalysis because of their intrinsic structural traits and intriguing electronic properties.[11, 248, 320] Examples of catalytic applications in environmental and energy related fields (see sections 3.1.3 and 3.2.1) have been discussed above. LDH-based materials have also been applied as catalysts (e.g., photocatalysts, Fenton catalysts, electrocatalysts, etc.) in many other fields, such as $CO_2$ reduction and oxygen evolution.[10, 299] Rather than introducing various catalytic applications of LDH-based materials, we focus on how to functionalize LDH catalysts herein. The key to functionalizing LDH catalysts is to address their poor electronic conductivity and limited active sites. Various aspects of LDHs can be regulated to achieve a high catalytic activity, including flexible regulation of the metal cations in the layers, overall morphology and pore structure, exchangeability of the intercalated anions in the interlayer space, availability of the interlayer space, accessibility of the functional species after hybridization (such as conductive materials, semiconductors, and noble metals or rare earth elements), and providential defect sites as suggested by **Section 2**. In summary, functionalization of LDH catalysts can be achieved via the modification of inner surface (interlayer), outer surface, and/or layers of LDHs.

Intercalating functional species into the interlayers of LDHs is one commonly used method to functionalize LDHs by addressing the issues of low electrical conductivity and low availability of the interlayer space. Various studies have demonstrated that catalytic activities of LDHs can be enhanced by introducing guest species into their interlayers.[321-324] For example, Long and coworkers intercalated graphene into the interlayers of NiFe-LDH to promote electron transport, which resulted in superior electrocatalytic properties of the resultant NiFe-LDH-graphene hybrids for oxygen evolution reaction with an overpotential as low as 210 mV.[324] Besides the strategy of intercalation of conductive materials, Li *et al*. found that the intercalation of formamide to expand the interlayer space of NiFe-LDH could promote the charge transfer of NiFe-LDH.[322] This is because the expanded interlayer provided more space for diffusion of the reactants, while more inner active sites could be available for reactions. Intercalation can also modify the surface electronic structure, improve electronic conductivity, and create more active sites for LDHs. These findings map out a promising strategy for further improving the activities of LDH catalysts by intercalating various guest species. But note that when intercalating functional species other than conductive materials as active sites, one should consider the space availability of the intercalated species, because the resultant narrow interlayer space may prevent the reactants from entering into the interlayer.

Functionalization via modification of outer surface can be achieved by hybridizing with conductive materials, semiconductors, noble metals/rare earth elements, or other functional species (see Section 2). But several aspects should be considered including but not limited to (i) size, morphology, and pore structure of the LDH-based catalysts. The decrease in size of the hybridized species, thickness and diversification of morphologies of LDHs, and the increase of porosity and specific surface area have significant impacts on the available active sites (including defect sites) and thus the electronic and catalytic properties of the LDH-based catalysts;[213-216, 219, 245] (ii) matching of the band structures of LDHs and the hybridized semiconductor when fabrication of heterojunctions. The perfect matching of the band structures can remarkably facilitate the transfer of photogenerated electron-hole pairs during the course of photocatalysis. As a result, the lifetime of electrons and holes is increased and the utilization of photogenic electrons and holes are effectively enhanced;[248, 325] (iii) high dispersion and high stability of active sites such as noble metals or rare earth elements. It is suggested that ordered distribution of the hybridized foreign species is important in optimizing photocatalytic activity of LDHs, and the chemical stability can also be significantly improved owing to the ordered structure between the LDH and the foreign species.[31] He *et al.* summarized this as the preferential orientation and dispersion issue of the active sites.[320] On the other hand, LDH catalysts can also be activated by modifying their layers. The most important characteristic of LDHs is that $M^{+1/2+}$ and $M'^{3+/4+}$ cations are distributed uniformly within the hydroxide layers.[326] By replacing the existing metal cations with more active metal elements and decreasing or reducing/oxidizing the existing metal cations, catalysts with a high activity and highly dispersive active sites can be produced.[26, 114, 187-189] In addition, active defect sites can also be introduced by these strategies.[26]

### 3.4 Biomaterials

There are extensive studies which indicate that 2D materials merit close attention in biomaterial applications, particularly in drug delivery and controlled release systems. The development of drug delivery systems with controlled release properties based on highly effective and safe carriers is pressing matters in medical research.[327, 328] Inorganic layers of 2D materials can confine drug molecules in their interspace and thus, drugs such as insulin or enzymes can be protected and gradually released, making 2D materials promising candidates for drug delivery and controlled release.[329] On the other hand, previous studies also indicated that the intercalation of drugs in the interlayers could reduce their toxicity and enhance bioavailability in a delivery process, which significantly reduced side effects.[330, 331] In addition to their interlayer sites, studies indicated that their outer surface can also be active sites to immobilize drug molecules.[332, 333]

2D LDHs are well known for their peculiar characteristics like good biocompatibility, anion exchange capacity, high chemical stability, and pH-dependent solubility.[327] These merits make them attractive and safe carriers for drug delivery and controlled release systems in biomaterial fields.[327, 334-337] The loading of drug molecules on LDHs endows LDHs to function in medical therapy. For example, Xu *et al.* intercalated pirenoxine sodium (PRN) and chitosan derivatives (chitosan-glutathione (CG), chitosan-glutathione-valine (CG-V), and chitosan-glutathione-valine-valine (CG-VV)) into the interlayers of MgAl-LDH, and found that the mean residence time and area under the curve ($AUC_{0-6h}$) of CG-PRN/LDH nanocomposite eye drop was respectively up to 2.1-fold and 6.3-fold higher than those of the commercial product of PRN during in vivo precorneal retention study on rabbits.[331] In addition, in vitro corneal penetration on rabbits demonstrated that the cumulative permeation of CG-VV-PRN/LDH nanocomposite dispersion was increased by 5.2 times compared to that of the commercial product. The authors indicated that the LDH-based

 

biomaterials presented prolonged precorneal retention, better corneal permeability, and enhanced ocular bioavailability compared to those of the commercial products.[331] Zhang *et al.* demonstrated that MgAl-LDHs were effective adjuvants for protein-based vaccines.[338] They assembled epitope peptides and CpG (cytosine-phosphate-guanine) onto the surface of LDH nanoparticles, and found that the tyrosinase-related protein 2 peptide functionalized LDH vaccine induced stronger cytotoxic T-lymphocyte responses and significantly inhibited the growth of tumor. Furthermore, the multi-target functionalized LDH vaccine by co-loading of tyrosinase-related protein 2, two mutated epitopes (M27 and M30), and CpG showed remarkable inhibition of melanoma growth. Their results suggested that LDHs are ideal platforms to load multi-antigens and immune stimulants as effective personalized therapeutic cancer vaccines. Kura *et al.* reported that the intercalated levodopa in the interlayers of LDHs could be released sequentially, controllably, slowly, and pH dependently with the release lasting for 3-6 days.[339] This slow releasing property of toxic compounds from the interlayers of LDHs over time is also a factor in suppressing drug toxicity.

Apart from as carries for drug delivery and controlled release systems, LDHs can also be applied in other medical fields such as tissue engineering implants,[340] antibacterial agents,[334, 341] medical imaging and targeted systems.[327] For example, Kapusetti *et al*. demonstrated that LDHs could be employed as bone cement for joint implants after hybridizing with poly(methyl methacrylate).[340] The bone cement showed superior mechanical strength, stiffness, toughness, fatigue resistance, and thermal stability in comparison with the pure bone cement. Peng *et al.* also confirmed the feasibility of using LDHs as bone implants.[342] Chen *et al*. functionalized an MgAl-LDH by hybridizing silver nanoparticles on the LDH, and found that the resultant material showed excellent antimicrobial activities against planktonic bacteria and inhibited the formation of biofilms.[341] Kuo *et al*. activated LDHs by modifying the external surface of LDHs with various organic groups and demonstrated that the resultant materials could enhance organ-specific targeting.[343] Their studies suggested that surface functionalization of LDH nanoparticles could promote drug targeting.

## 4 Summary and outlook

In this review, we have addressed the currently available strategies to functionalize LDHs and discussed how these strategies may improve a range of physicochemical properties of LDHs. Currently available functionalization strategies include intercalation, surface modification, hybridization, layered compositions regulation, size and morphology control, and defect creation. We have documented how these strategies contribute significantly to the improvement of a very diverse range of physicochemical responses of an LDH, including adsorptive, catalytic, electronic, electrochemical, and optic performances. The remarkable performances endow functionalized LDHs with great potential across a wide range of applications in the environmental remediation, energy, catalysis, and biomaterial sectors. We have highlighted their potential applications in these fields.

Functionalization of LDHs continues to be a rapidly growing field. We believe future studies could be rewarded by focusing efforts on several fundamental research areas, including:

(i) Using computer modeling to help gain a deeper understanding of LDH functionalization, which will facilitate more effective functionalization of LDHs. To this end, the biggest challenge is to set up proper models for simulation since different functionalization methods may not share a same model.

(ii) New and effective nano-hybridization routes. As both decreasing the size of LDHs and hybridizing LDHs with guest species can lead to dramatic performance improvement of LDHs, the hybridization at the nanoscale may induce new features. Conventionally, ultrathin 2D LDH-based nanomaterials are prepared based on exfoliation technologies followed by layer-by-layer and one-step coassembly methods. But the current exfoliation technologies considerably inhibit the fabrication of large scale and high quality ultrathin 2D LDH-based nanomaterials due to the low exfoliation yield and poor controllability. Therefore, from the material synthesis point of view, the current quality, production rate, and production yield of ultrathin 2D LDH-based nanomaterials are still far from commercialization. One of the major challenges in this hot field is to realize high-yield and massive production of ultrathin 2D nanomaterials to meet the industry requirements. The development of in-situ and/or one-pot synthesis strategies for ultrathin 2D LDH-based hybrid nanomaterials should be one of the future research targets.

(iii) Achieving ordered intercalation and hybridization. The remaining challenges are to maintain the arrangement of the guest species hybridized onto LDHs with defined orientation, to direct the guest species to a spatially defined region, and to order multiple guests on LDH surfaces. Taking functionalization of LDHs by intercalation as an example, key future studies to be conducted include development of more facile intercalation approaches, especially for two or more co-intercalated guest species, as well as further studies over the basic factors that affect intercalation. Intercalation can remarkably enhance the physical and chemical properties of LDHs, rendering LDH materials favorable for a multitude of vital applications. In addition, co-intercalation of different intercalants into one 2D material has been shown to lead to unpredicted properties compared to single matter intercalated LDHs.[1] Thus, multi-functional species intercalation may give rise to new synergistic properties that are unprecedented with single intercalants. To achieve this goal, more efficient intercalation methods as well as further exploration of the influential factors of co-intercalation are needed. During co-intercalation, the controlled loading of different functional substances at various ratios, stacking forms, and relative position of the functional substances in the LDH layers are key challenge. The intercalation order, intercalation medium, and interactions among different functional species and LDH layers are expected to significantly affect the intercalation process and outcome.

(iv) Investigation of defect structures and linking these to specific LDH functions. Creation of defects is a theoretically and practically viable and promising approach to functionalize LDHs, but the challenge is how to create controllable defects. In addition, it is also critical to identify which type of defects is beneficial or harmful to the specific performance of LDHs. Importantly, how to avoid unfavorable defects and introduce useful defect sites are the biggest challenges for the future researches.

(v) New generation of LDH-based electrochemical energy storage materials. For example, if LDHs can be efficiently developed to serve as the host matrix for the intercalation of

various earth-abundant cations, a new family of electrochemical energy storage materials can be developed. However, owing to the occupation of the interlayer gallery by anions and the charge repulsion between the positively charged LDH laminate and cations, the intercalation of cations from aqueous solution into the domain of LDHs becomes the major difficulty for the fabrication of this new type of energy storage materials. Recent breakthrough was made by the creation of ordered hydrogen-vacancy on CoFe-LDH, and therefore various metal cations (e.g., $Li^+$, $Na^+$, $K^+$, $Ca^{2+}$, $Mg^{2+}$, and $Zn^{2+}$) could be intercalated into the interlayers of CoFe-LDH, resulting in high-performance rechargeable cation supercapacitors.[344] More efforts should be directed to this new area.

## Conflicts of interest

There are no conflicts to declare.

## Acknowledgements

L.S. acknowledges the support from the National Science Foundation (CMMI-1562907). R.Z. acknowledges the support from the National Natural Science Foundation of China (41572031). D.O. acknowledges the support from SCG Chemicals Co. Ltd. M.L. thanks the National Natural Science Foundation of China (41902039), and the China Scholarship Council for offering him a scholarship to conduct research at University of Connecticut.

## References

1. J. Wan, S. D. Lacey, J. Dai, W. Bao, M. S. Fuhrer and L. Hu, Chem. Soc. Rev., 2016, 45, 6742-6765.
2. L. Ma, Q. Wang, S. M. Islam, Y. Liu, S. Ma and M. G. Kanatzidis, J. Am. Chem. Soc., 2016, 138, 2858-2866.
3. S. Ma, L. Huang, L. Ma, Y. Shim, S. M. Islam, P. Wang, L.-D. Zhao, S. Wang, G. Sun and X. Yang, J. Am. Chem. Soc., 2015, 137, 3670-3677.
4. Q. Tao, B. J. Reddy, H. He, R. L. Frost, P. Yuan and J. Zhu, Mater. Chem. Phys., 2008, 112, 869-875.
5. Q. Tao, Y. Zhang, X. Zhang, P. Yuan and H. He, J. Solid State Chem., 2006, 179, 708-715.
6. J. Yu, Q. Wang, D. O'Hare and L. Sun, Chem. Soc. Rev., 2017.
7. Q. Tao, H. He, R. L. Frost, P. Yuan and J. Zhu, Appl. Surf. Sci., 2009, 255, 4334-4340.
8. Y. Zhu, M. Laipan, R. Zhu, T. Xu, J. Liu, J. Zhu, Y. Xi, G. Zhu and H. He, Molecular Catalysis, 2017, 427, 54-61.
9. C. Li, M. Wei, D. G. Evans and X. Duan, Small, 2014, 10, 4469-4486.
10. L. Mohapatra and K. Parida, Journal of Materials Chemistry A, 2016, 4, 10744-10766.
11. Q. Wang and D. O'Hare, Chem. Rev., 2012, 112, 4124-4155.
12. Q.-S. Yao, Z.-C. Li, Z.-M. Qiu, F. Zhang, X.-B. Chen, D.-C. Chen, S.-K. Guan and R.-C. Zeng, Rare Met. , 2019, 38, 629-641.
13. M. Laipan, R. Zhu, J. Zhu and H. He, J. Mol. Catal. A: Chem., 2016, 415, 9-16.
14. L. Yu, H. Zhou, J. Sun, F. Qin, F. Yu, J. Bao, Y. Yu, S. Chen and Z. Ren, Energy Environ. Sci. , 2017, 10, 1820-1827.
15. G. Nagaraju, G. S. R. Raju, Y. H. Ko and J. S. Yu, Nanoscale, 2016, 8, 812-825.
16. Y. Ao, D. Wang, P. Wang, C. Wang, J. Hou and J. Qian, RSC Advances, 2015, 5, 54613-54621.
17. S. Mancipe, F. Tzompantzi and R. Gómez, Appl. Clay Sci., 2017, 136, 67-74.
18. J. Zhu, P. Yuan, H. He, R. Frost, Q. Tao, W. Shen and T. Bostrom, J. Colloid Interface Sci., 2008, 319, 498-504.
19. W. Guan, S. Wang, C. Lu and B. Z. Tang, Nature communications, 2016, 7.
20. X. Gao, X. Liu, D. Wu, B. Qian, Z. Kou, Z. Pan, Y. Pang, L. Miao and J. Wang, Adv. Funct. Mater., 2019, 29.
21. B. Wang, H. Zhang, D. G. Evans and X. Duan, Mater. Chem. Phys., 2005, 92, 190-196.
22. J. Wang, Y. Zhang, J. Zhu, J. Hou, J. Liu and B. Van der Bruggen, J. Membr. Sci., 2016, 510, 27-37.
23. F. Ning, M. Shao, S. Xu, Y. Fu, R. Zhang, M. Wei, D. G. Evans and X. Duan, Energy Environ. Sci. , 2016, 9, 2633-2643.
24. Z. Gu, J. J. Atherton and Z. P. Xu, Chem. Commun., 2015, 51, 3024-3036.
25. M. Gong, Y. Li, H. Zhang, B. Zhang, W. Zhou, J. Feng, H. Wang, Y. Liang, Z. Fan and J. Liu, Energy Environ. Sci. , 2014, 7, 2025-2032.
26. H. Liu, Y. Wang, X. Lu, Y. Hu, G. Zhu, R. Chen, L. Ma, H. Zhu, Z. Tie and J. Liu, Nano Energy, 2017, 35, 350-357.
27. Y. Zhao, Q. Wang, T. Bian, H. Yu, H. Fan, C. Zhou, L.-Z. Wu, C.-H. Tung, D. O'Hare and T. Zhang, Nanoscale, 2015, 7, 7168-7173.
28. F. Yang, B. Wang, H. Su, S. Zhou and Y. Kong, Materials Chemistry Frontiers, 2017.
29. J. L. Gunjakar, I. Y. Kim, J. M. Lee, N.-S. Lee and S.-J. Hwang, Energy Environ. Sci. , 2013, 6, 1008-1017.
30. M. Shao, M. Wei, D. G. Evans and X. Duan, Chemistry-A European Journal, 2013, 19, 4100-4108.
31. J. L. Gunjakar, T. W. Kim, H. N. Kim, I. Y. Kim and S.-J. Hwang, J. Am. Chem. Soc., 2011, 133, 14998-15007.
32. M. Yu, S. Zhou, Z. Wang, J. Zhao and J. Qiu, Nano Energy, 2018, 44, 181-190.
33. J. Xu, S. Gai, F. He, N. Niu, P. Gao, Y. Chen and P. Yang, Journal of Materials Chemistry A, 2014, 2, 1022-1031.
34. C. Yu, J. Yang, C. Zhao, X. Fan, G. Wang and J. Qiu, Nanoscale, 2014, 6, 3097-3104.
35. H. Hu, X. Wang, S. Xu, W. Yang, F. Xu, J. Shen and C. Mao, J. Mater. Chem., 2012, 22, 15362-15369.
36. H. Hu, K. Xiu, S. Xu, W. Yang and F. Xu, Bioconjugate Chem., 2013, 24, 968-978.
37. C. I. Ezeh, X. Huang, X. Yang, C.-g. Sun and J. Wang, Ultrason. Sonochem., 2017, 39, 330-343.
38. Y. Xu, W. Huang, X. Chen, F. Ge, R. Zhu and L. Sun, Appl. Catal., A 2018, 550, 8.
39. L. Zhang, K. N. Hui, K. San Hui and H. Lee, Electrochim. Acta, 2015, 186, 522-529.
40. J. Cheng, J. Fang, M. Li, W. Zhang, F. Liu and X. Zhang, Electrochim. Acta, 2013, 114, 68-75.
41. F. Lai, Y. Huang, Y.-E. Miao and T. Liu, Electrochim. Acta, 2015, 174, 456-463.
42. M. Tian, C. Liu, Z. G. Neale, J. Zheng, D. Long and G. Cao, ACS Appl. Mat. Interfaces 2019, 11, 35977-35986.
43. S. Fu, G. Fan, L. Yang and F. Li, Electrochim. Acta, 2015, 152, 146-154.
44. X. Han, C. Yu, J. Yang, C. Zhao, H. Huang, Z. Liu, P. M. Ajayan and J. Qiu, Adv. Mater. Interfaces, 2016, 3.

 

45. C. Yu, X. Han, Z. Liu, C. Zhao, H. Huang, J. Yang, Y. Niu and J. Qiu, Carbon, 2018, 126, 437-442.
46. J. W. Mellor, Nature (London, U. K.), 1917, 100, 88-89.
47. A. Weiss and A. Weiss, Angew. Chem., 1960, 72, 413-415.
48. D. W. Bruce, D. O'Hare and Editors, Inorganic Materials, Wiley, 1992.
49. K. Fredenhagen and G. Cadenbach, Z. Anorg. Allg. Chem., 1926, 158, 249-263.
50. A. Clearfield, in Progress in Intercalation Research, eds. W. Müller-Warmuth and R. Schöllhorn, Kluwer Academic Publisher, Dordrecht, The Netherlands, 1994, pp. 240-263.
51. D. O'Hare, in Inorg. Mater. , eds. D. W. Bruce and D. O'Hare, John Wiley & Sons, West Sussex, 1992, pp. 165-235.
52. A. Clearfield and U. Costantino, in Comprehensive Supramolecular Chemistry, eds. G. Alberti and T. Bein, Elsevier, Oxford, UK, 1996, vol. 7, pp. 107-149.
53. J. Yu, L. Xiang, B. R. Martin, A. Clearfield and L. Sun, Chem. Commun., 2015, 51, 11398-11400.
54. J. Yu, J. E. Sims and L. Sun, J. Mater. Sci., 2017, 52, 6647-6655.
55. M. Laipan, H. Fu, R. Zhu, L. Sun, J. Zhu and H. He, Scientific Reports, 2017, 7.
56. M. Laipan, R. Zhu, Q. Chen, J. Zhu, Y. Xi, G. A. Ayoko and H. He, J. Hazard. Mater., 2015, 300, 572-580.
57. W. J. Boo, L. Sun, J. Liu, A. Clearfield and H.-J. Sue, J. Phys. Chem. C, 2007, 111, 10377-10381.
58. H. Hu, J. C. Martin, M. Xiao, C. S. Southworth, Y. Meng and L. Sun, J. Phys. Chem. C, 2011, 115, 5509-5514.
59. L. Sun, J. Y. O'Reilly, D. Kong, J. Y. Su, W. J. Boo, H. J. Sue and A. Clearfield, J. Colloid Interface Sci., 2009, 333, 503-509.
60. H. He, L. Ma, J. Zhu, R. L. Frost, B. K. Theng and F. Bergaya, Appl. Clay Sci., 2014, 100, 22-28.
61. J. Zhu, K. Wen, P. Zhang, Y. Wang, L. Ma, Y. Xi, R. Zhu, H. Liu and H. He, Microporous Mesoporous Mater., 2017, 242, 256-263.
62. J. Zhu, P. Zhang, Y. Qing, K. Wen, X. Su, L. Ma, J. Wei, H. Liu, H. He and Y. Xi, Appl. Clay Sci., 2017, 141, 265-271.
63. Q. Tao, J. Zhu, R. L. Frost, T. E. Bostrom, R. M. Wellard, J. Wei, P. Yuan and H. He, Langmuir, 2009, 26, 2769-2773.
64. S. M. Xu, Q. C. Zhu, J. Long, H. H. Wang, X. F. Xie, K. X. Wang and J. S. Chen, Adv. Funct. Mater., 2016, 26, 1365-1374.
65. S. Omwoma, W. Chen, R. Tsunashima and Y.-F. Song, Coord. Chem. Rev., 2014, 258, 58-71.
66. L. Ma, S. M. Islam, C. Xiao, J. Zhao, H. Liu, M. Yuan, G. Sun, H. Li, S. Ma and M. G. Kanatzidis, J. Am. Chem. Soc., 2017, 139, 12745-12757.
67. Q. Zhou, F. Chen, W. Wu, R. Bu, W. Li and F. Yang, Chem. Eng. J., 2016, 285, 198-206.
68. N. Wang, J. Sun, H. Fan and S. Ai, Talanta, 2016, 148, 301-307.
69. Y. Jia, Y. Fang, Y. Zhang, H. N. Miras and Y. F. Song, Chemistry-A European Journal, 2015, 21, 14862-14870.
70. Y. Chen, Z. Yao, H. N. Miras and Y. F. Song, Chemistry-A European Journal, 2015, 21, 10812-10820.
71. W. Lv, L. Yang, B. Fan, Y. Zhao, Y. Chen, N. Lu and R. Li, Chem. Eng. J., 2015, 263, 309-316.
72. M. Asif, A. Aziz, A. Q. Dao, A. Hakeem, H. Wang, S. Dong, G. Zhang, F. Xiao and H. Liu, Anal. Chim. Acta, 2015, 898, 34-41.
73. F.-N. Xiao, K. Wang, F.-B. Wang and X.-H. Xia, Anal. Chem., 2015, 87, 4530-4537.
74. J. Wu, D. Peng, Y. He, X. Du, Z. Zhang, B. Zhang, X. Li and Y. Huang, Materials, 2017, 10, 426.
75. Y. Zhao, H. Hu, X. Yang, D. Yan and Q. Dai, Small, 2016, 12, 4471-4476.
76. H. Asiabi, Y. Yamini, M. Shamsayei and E. Tahmasebi, Chem. Eng. J., 2017, 323, 212-223.
77. A. C. Thenuwara, N. H. Attanayake, J. Yu, J. P. Perdew, E. J. Elzinga, Q. Yan and D. R. Strongin, The Journal of Physical Chemistry B, 2017.
78. C. Zhang, T. Tsuboi, H. Namba, Y. Einaga and T. Yamamoto, Dalton Trans., 2016, 45, 13324-13331.
79. C. Wang, X. Zhang, Z. Xu, X. Sun and Y. Ma, ACS Appl. Mat. Interfaces 2015, 7, 19601-19610.
80. W. Quan, C. Jiang, S. Wang, Y. Li, Z. Zhang, Z. Tang and F. Favier, Electrochim. Acta, 2017, 247, 1072-1079.
81. J. M. Oh, S. J. Choi, G. E. Lee, S. H. Han and J. H. Choy, Adv. Funct. Mater., 2009, 19, 1617-1624.
82. L. Li, G. Qi, B. Wang, D. Yue, Y. Wang and T. Sato, J. Hazard. Mater., 2018, 343, 19-28.
83. E. Lima, M. a. d. J. s. Martínez-Ortiz, R. I. G. r. Reyes and M. Vera, Inorg. Chem., 2012, 51, 7774-7781.
84. A. M. El-Toni, M. A. Habila, J. P. Labis, Z. A. ALOthman, M. Alhoshan, A. A. Elzatahry and F. Zhang, Nanoscale, 2016, 8, 2510-2531.
85. M. Shao, F. Ning, Y. Zhao, J. Zhao, M. Wei, D. G. Evans and X. Duan, Chem. Mater., 2012, 24, 1192-1197.
86. R. G. Chaudhuri and S. Paria, Chem. Rev, 2012, 112, 2373-2433.
87. J. Han, Y. Dou, J. Zhao, M. Wei, D. G. Evans and X. Duan, Small, 2013, 9, 98-106.
88. M. B. Gawande, A. Goswami, T. Asefa, H. Guo, A. V. Biradar, D.-L. Peng, R. Zboril and R. S. Varma, Chem. Soc. Rev., 2015, 44, 7540-7590.
89. M. Asif, H. Liu, A. Aziz, H. Wang, Z. Wang, M. Ajmal, F. Xiao and H. Liu, Biosens. Bioelectron., 2017.
90. Y. Li, H.-Y. Bi, H. Li, X.-M. Mao and Y.-Q. Liang, Materials Science and Engineering: C, 2017, 78, 886-891.
91. L.-g. Yan, K. Yang, R.-r. Shan, T. Yan, J. Wei, S.-j. Yu, H.-q. Yu and B. Du, J. Colloid Interface Sci., 2015, 448, 508-516.
92. X. Li, Z. Yang, W. Qi, Y. Li, Y. Wu, S. Zhou, S. Huang, J. Wei, H. Li and P. Yao, Appl. Surf. Sci., 2016, 363, 381-388.
93. X. He, Q. Liu, J. Liu, R. Li, H. Zhang, R. Chen and J. Wang, J. Alloys Compd., 2017, 724, 130-138.
94. Q. Guo, Q. Zhang, H. Wang, Z. Liu and Z. Zhao, Catal. Commun., 2016, 77, 118-122.
95. Z. Li, M. Shao, L. Zhou, R. Zhang, C. Zhang, J. Han, M. Wei, D. G. Evans and X. Duan, Nano Energy, 2016, 20, 294-304.
96. W. Chen, T. Wang, J. Xue, S. Li, Z. Wang and S. Sun, Small, 2017, 13.
97. X. Zhou, X. Wang, R. Tong, L. Xiao, Z. Zheng, X. Peng, H. Wang and H. Wang, Int. J. Energy Res. , 2017.
98. C. Wang, B. Ma, S. Xu, D. Li, S. He, Y. Zhao, J. Han, M. Wei, D. G. Evans and X. Duan, Nano Energy, 2017, 32, 463-469.
99. A. S. Oliveira, A. C. Alcântara and S. B. Pergher, Materials Science and Engineering: C, 2017, 75, 1250-1258.

100. X. Fan, B. Gao, T. Wang, X. Huang, H. Gong, H. Xue, H. Guo, L. Song, W. Xia and J. He, Appl. Catal., A 2016, 528, 52-58.
101. Y. Zhu, J. Ren, X. Yang, G. Chang, Y. Bu, G. Wei, W. Han and D. Yang, Journal of Materials Chemistry A, 2017, 5, 9952-9959.
102. Y. Wang, Y. Zhou, T. Zhang, M. He and X. Bu, Chem. Eng. J., 2015, 266, 199-202.
103. C. Chen, R. Felton, J.-C. Buffet and D. O'Hare, Chem. Commun., 2015, 51, 3462-3465.
104. L. Guo, X. Zhang, Q. Chen, C. Ruan and Y. Leng, Environmental Science and Pollution Research, 2016, 23, 6749-6757.
105. J. Xing, J. Du, X. Zhang, Y. Shao, T. Zhang and C. Xu, Dalton Trans., 2017, 46, 10064-10072.
106. S. Wang, Z. Huang, R. Li, X. Zheng, F. Lu and T. He, Electrochim. Acta, 2016, 204, 160-168.
107. Q. Zhou, M. Lei, J. Li, K. Zhao and Y. Liu, Sep. Purif. Technol., 2017, 182, 78-86.
108. L. Yu, H. Zhou, J. Sun, F. Qin, D. Luo, L. Xie, F. Yu, J. Bao, Y. Li and Y. Yu, Nano Energy, 2017.
109. Y. Ni, L. Yao, Y. Wang, B. Liu, M. Cao and C. Hu, Nanoscale, 2017, 9, 11596-11604.
110. J. Xu, C. Ma, J. Cao and Z. Chen, Dalton Trans., 2017, 46, 3276-3283.
111. S. Wu, K. S. Hui, K. N. Hui and K. H. Kim, ACS Appl. Mat. Interfaces 2016, 9, 1395-1406.
112. P.-F. Liu, K. Tao, G.-C. Li, M.-K. Wu, S.-R. Zhu, F.-Y. Yi, W.-N. Zhao and L. Han, Dalton Trans., 2016, 45, 12632-12635.
113. H. Ma, J. He, D.-B. Xiong, J. Wu, Q. Li, V. Dravid and Y. Zhao, ACS Appl. Mat. Interfaces 2016, 8, 1992-2000.
114. S. Zhang, J. Liu, P. Huang, H. Wang, C. Cao and W. Song, Science Bulletin, 2017.
115. A. N. Ay, H. Akar, A. Zaulet, C. Viňas, F. Teixidor and B. Zumreoglu-Karan, Dalton Trans., 2017, 46, 3303-3310.
116. L. Qian, W. Zhang, J. Yan, L. Han, Y. Chen, D. Ouyang and M. Chen, Environ. Pollut., 2017, 223, 153-160.
117. W. Zhu, L. Liu, Z. Yue, W. Zhang, X. Yue, J. Wang, S. Yu, L. Wang and J. Wang, ACS Appl. Mat. Interfaces 2017.
118. Y. Tao, L. Ruiyi, Y. Tingting and L. Zaijun, Electrochim. Acta, 2015, 152, 530-537.
119. J. Yang, C. Yu, X. Fan, Z. Ling, J. Qiu and Y. Gogotsi, J. Mater. Chem. A, 2013, 1, 1963-1968.
120. Z. Liu, C. Yu, X. Han, J. Yang, C. Zhao, H. Huang and J. Qiu, ChemElectroChem, 2016, 3, 906-912.
121. K. Le, Z. Wang, F. Wang, Q. Wang, Q. Shao, V. Murugadoss, S. Wu, W. Liu, J. Liu and Q. Gao, Dalton Trans., 2019, 48, 5193-5202.
122. X. Liu, C. Wang, Y. Dou, A. Zhou, T. Pan, J. Han and M. Wei, Journal of Materials Chemistry A, 2014, 2, 1682-1685.
123. J. Yang, C. Yu, C. Hu, M. Wang, S. Li, H. Huang, K. Bustillo, X. Han, C. Zhao and W. Guo, Adv. Funct. Mater., 2018, 28, 1803272.
124. Y. Tang, R. Wang, Y. Yang, D. Yan and X. Xiang, ACS Appl. Mat. Interfaces 2016, 8, 19446-19455.
125. G. Zhang, B. Lin, Y. Qiu, L. He, Y. Chen and B. Gao, Int. J. Hydrogen Energy, 2015, 40, 4758-4765.
126. G. Mikami, F. Grosu, S. Kawamura, Y. Yoshida, G. Carja and Y. Izumi, Appl. Catal., B 2016, 199, 260-271.
127. X. Cai, X. Shen, L. Ma, Z. Ji, C. Xu and A. Yuan, Chem. Eng. J., 2015, 268, 251-259.
128. F. Lai, Y. E. Miao, L. Zuo, H. Lu, Y. Huang and T. Liu, Small, 2016, 12, 3235-3244.
129. C. Wang, X. Zhang, X. Sun and Y. Ma, Electrochim. Acta, 2016, 191, 329-336.
130. C. Xing, F. Musharavati, H. Li, E. Zalezhad, O. K. Hui, S. Bae and B.-Y. Cho, RSC Advances, 2017, 7, 38945-38950.
131. X. Bai, Q. Liu, H. Zhang, J. Liu, Z. Li, X. Jing, Y. Yuan, L. Liu and J. Wang, Electrochim. Acta, 2016, 215, 492-499.
132. F. Wang, S. Sun, Y. Xu, T. Wang, R. Yu and H. Li, Scientific Reports, 2017, 7.
133. X. Yu, M. Zhang, W. Yuan and G. Shi, Journal of Materials Chemistry A, 2015, 3, 6921-6928.
134. W. Ma, R. Ma, C. Wang, J. Liang, X. Liu, K. Zhou and T. Sasaki, ACS Nano, 2015, 9, 1977-1984.
135. R. Chen, G. Sun, C. Yang, L. Zhang, J. Miao, H. Tao, H. Yang, J. Chen, P. Chen and B. Liu, Nanoscale Horizons, 2016, 1, 156-160.
136. D. H. Youn, Y. B. Park, J. Y. Kim, G. Magesh, Y. J. Jang and J. S. Lee, J. Power Sources, 2015, 294, 437-443.
137. Y. Lu, B. Jiang, L. Fang, F. Ling, F. Wu, B. Hu, F. Meng, K. Niu, F. Lin and H. Zheng, J. Alloys Compd., 2017, 714, 63-70.
138. M. Li, F. Liu, J. Cheng, J. Ying and X. Zhang, J. Alloys Compd., 2015, 635, 225-232.
139. L. Zhang, R. Chen, K. N. Hui, K. San Hui and H. Lee, Chem. Eng. J., 2017.
140. L. Zhang, K. N. Hui, K. San Hui and H. Lee, J. Power Sources, 2016, 318, 76-85.
141. X. Ge, C. Gu, Z. Yin, X. Wang, J. Tu and J. Li, Nano Energy, 2016, 20, 185-193.
142. L. Zhang, K. Hui, K. Hui, X. Chen, R. Chen and H. Lee, Int. J. Hydrogen Energy, 2016, 41, 9443-9453.
143. B. Hai and Y. Zou, Sens. Actuators, B 2015, 208, 143-150.
144. Y. Wang, H. Dou, J. Wang, B. Ding, Y. Xu, Z. Chang and X. Hao, J. Power Sources, 2016, 327, 221-228.
145. P. Huang, C. Cao, Y. Sun, S. Yang, F. Wei and W. Song, Journal of Materials Chemistry A, 2015, 3, 10858-10863.
146. C.-H. Zheng, T. Yao, T.-R. Xu, H.-A. Wang, P.-F. Huang, Y. Yan and D.-L. Fang, J. Alloys Compd., 2016, 678, 93-101.
147. X. L. Guo, X. Y. Liu, X. D. Hao, S. J. Zhu, F. Dong, Z. Q. Wen and Y. X. Zhang, Electrochim. Acta, 2016, 194, 179-186.
148. H. Chen, Y. Ai, F. Liu, X. Chang, Y. Xue, Q. Huang, C. Wang, H. Lin and S. Han, Electrochim. Acta, 2016, 213, 55-65.
149. M. Yu, R. Liu, J. Liu, S. Li and Y. Ma, Small, 2017.
150. W. Ma, R. Ma, J. Wu, P. Sun, X. Liu, K. Zhou and T. Sasaki, Nanoscale, 2016, 8, 10425-10432.
151. L. Huang, B. Liu, H. Hou, L. Wu, X. Zhu, J. Hu and J. Yang, J. Alloys Compd., 2017.
152. M. Padmini, S. K. Kiran, N. Lakshminarasimhan, M. Sathish and P. Elumalai, Electrochim. Acta, 2017, 236, 359-370.
153. M. Li, J. Cheng, J. Wang, F. Liu and X. Zhang, Electrochim. Acta, 2016, 206, 108-115.
154. J. Ping, Y. Wang, Q. Lu, B. Chen, J. Chen, Y. Huang, Q. Ma, C. Tan, J. Yang and X. Cao, Adv. Mater. , 2016, 28, 7640-7645.
155. A. Zhang, C. Wang, Q. Xu, H. Liu, Y. Wang and Y. Xia, Rsc Advances, 2015, 5, 26017-26026.
156. W. Peng, H. Li and S. Song, ACS Appl. Mat. Interfaces 2017, 9, 5204-5212.
157. Z. Huang, S. Wang, J. Wang, Y. Yu, J. Wen and R. Li, Electrochim. Acta, 2015, 152, 117-125.

158. K. Ma, J. Cheng, F. Liu and X. Zhang, J. Alloys Compd., 2016, 679, 277-284.
159. J. Hu, C. Zhang, L. Jiang, H. Lin, Y. An, D. Zhou, M. K. Leung and S. Yang, Joule, 2017, 1, 383-393.
160. R. Zhang, M. Shao, S. Xu, F. Ning, L. Zhou and M. Wei, Nano Energy, 2017, 33, 21-28.
161. L. Mohapatra, D. Patra, K. Parida and S. J. Zaidi, Eur. J. Inorg. Chem., 2017, 2017, 723-733.
162. M. Mureseanu, T. Radu, R.-D. Andrei, M. Darie and G. Carja, Appl. Clay Sci., 2017, 141, 1-12.
163. Z. Li, M. Chen, Q. Zhang, J. Qu, Z. Ai and Y. Li, Appl. Clay Sci., 2017, 144, 115-120.
164. M. Hadnadjev-Kostic, T. Vulic, R. Marinkovic-Neducin, D. Lončarević, J. Dostanić, S. Markov and D. Jovanović, Journal of Cleaner Production, 2017, 164, 1-18.
165. T. Vulic, O. Rudic, S. Vucetic, D. Lazar and J. Ranogajec, Cem. Concr. Compos. , 2015, 58, 50-58.
166. Y. Hou, Z. Wen, S. Cui, X. Feng and J. Chen, Nano Lett., 2016, 16, 2268-2277.
167. S. Nayak, L. Mohapatra and K. Parida, Journal of Materials Chemistry A, 2015, 3, 18622-18635.
168. J. Ma, J. Ding, L. Yu, L. Li, Y. Kong and S. Komarneni, Appl. Clay Sci., 2015, 109, 76-82.
169. Z. Wang, S. Zeng, W. Liu, X. Wang, Q. Li, Z. Zhao and F. Geng, ACS Appl. Mat. Interfaces 2017, 9, 1488-1495.
170. S. Kumar, M. A. Isaacs, R. Trofimovaite, L. Durndell, C. M. Parlett, R. E. Douthwaite, B. Coulson, M. C. Cockett, K. Wilson and A. F. Lee, Appl. Catal., B 2017, 209, 394-404.
171. Y. Fu, F. Ning, S. Xu, H. An, M. Shao and M. Wei, Journal of Materials Chemistry A, 2016, 4, 3907-3913.
172. K. Mori, T. Taga and H. Yamashita, ACS Catalysis, 2017, 7, 3147-3151.
173. E. Seftel, M. Puscasu, M. Mertens, P. Cool and G. Carja, Appl. Catal., B 2015, 164, 251-260.
174. S. Nayak and K. Parida, Int. J. Hydrogen Energy, 2016, 41, 21166-21180.
175. Y. Chen, Y. Bao and X. Wang, Journal of fluorescence, 2016, 26, 813-820.
176. X. Jin, Y. Koizumi, K. Yamaguchi, K. Nozaki and N. Mizuno, J. Am. Chem. Soc., 2017.
177. S. M. de Rezende, C. A. Franchini, M. L. Dieuzeide, A. M. D. de Farias, N. Amadeo and M. A. Fraga, Chem. Eng. J., 2015, 272, 108-118.
178. K. Iqbal, A. Iqbal, A. M. Kirillov, B. Wang, W. Liu and Y. Tang, Journal of Materials Chemistry A, 2017, 5, 6716-6724.
179. L. Sobhana, M. Sarakha, V. Prevot and P. Fardim, Appl. Clay Sci., 2016, 134, 120-127.
180. Z. Gao, R. Xie, G. Fan, L. Yang and F. Li, ACS Sustainable Chemistry & Engineering, 2017.
181. M. Suarez-Quezada, G. Romero-Ortiz, V. Suárez, G. Morales-Mendoza, L. Lartundo-Rojas, E. Navarro-Cerón, F. Tzompantzi, S. Robles, R. Gómez and A. Mantilla, Catal. Today, 2016, 271, 213-219.
182. Y. Zhu, R. Zhu, G. Zhu, M. Wang, Y. Chen, J. Zhu, Y. Xi and H. He, Appl. Surf. Sci., 2017.
183. S. Kawamura, M. C. Puscasu, Y. Yoshida, Y. Izumi and G. Carja, Appl. Catal., A 2015, 504, 238-247.
184. Y. Wei, S. Chen, F. Li, Y. Lin, Y. Zhang and L. Liu, ACS Appl. Mat. Interfaces 2015, 7, 14182-14191.
185. X. Duan and D. G. Evans, Layered double hydroxides, Springer Science & Business Media, 2006.
186. J. Liang, R. Ma, N. Iyi, Y. Ebina, K. Takada and T. Sasaki, Chem. Mater., 2009, 22, 371-378.
187. Z. Lu, L. Qian, Y. Tian, Y. Li, X. Sun and X. Duan, Chem. Commun., 2016, 52, 908-911.
188. X. Li, M. Xin, S. Guo, T. Cai, D. Du, W. Xing, L. Zhao, W. Guo, Q. Xue and Z. Yan, Electrochim. Acta, 2017, 253, 302-310.
189. K. Parida, M. Satpathy and L. Mohapatra, J. Mater. Chem., 2012, 22, 7350-7357.
190. T. Kameda, E. Kondo and T. Yoshioka, Sep. Purif. Technol., 2014, 122, 12-16.
191. X. Wang, Y. Lin, Y. Su, B. Zhang, C. Li, H. Wang and L. Wang, Electrochim. Acta, 2017, 225, 263-271.
192. M. Dinari, M. M. Momeni and Y. Ghayeb, J. Mater. Sci.: Mater. Electron., 2016, 27, 9861-9869.
193. S. Kim, J. Fahel, P. Durand, E. André and C. Carteret, Eur. J. Inorg. Chem., 2017, 2017, 669-678.
194. K. Grover, S. Komarneni and H. Katsuki, Appl. Clay Sci., 2010, 48, 631-637.
195. M. Sui, Y. Zhou, L. Sheng and B. Duan, Chem. Eng. J., 2012, 210, 451-460.
196. S. Kim, S. G. Jeon and K. B. Lee, ACS Appl. Mat. Interfaces 2016, 8, 5763-5767.
197. E. Dore and F. Frau, Environmental Science and Pollution Research, 2017, 1-14.
198. T. Lv, W. Ma, G. Xin, R. Wang, J. Xu, D. Liu, F. Liu and D. Pan, J. Hazard. Mater., 2012, 237, 121-132.
199. A. A. A. Ahmed, Z. A. Talib, M. Z. bin Hussein and A. Zakaria, J. Solid State Chem., 2012, 191, 271-278.
200. Y. Yang, X. Yan, X. Hu, R. Feng and M. Zhou, J. Colloid Interface Sci., 2017.
201. M. Shao, J. Han, M. Wei, D. G. Evans and X. Duan, Chem. Eng. J., 2011, 168, 519-524.
202. Y. Zhao, B. Li, Q. Wang, W. Gao, C. J. Wang, M. Wei, D. G. Evans, X. Duan and D. O'Hare, Chemical Science, 2014, 5, 951-958.
203. L.-J. Zhou, X. Huang, H. Chen, P. Jin, G.-D. Li and X. Zou, Dalton Trans., 2015, 44, 11592-11600.
204. J. Zhang, J. Cheng, M. Li, L. Liu, F. Liu and X. Zhang, J. Electroanal. Chem., 2015, 743, 38-45.
205. A. Sumboja, J. Chen, Y. Zong, P. S. Lee and Z. Liu, Nanoscale, 2017, 9, 774-780.
206. F. Ling, L. Fang, Y. Lu, J. Gao, F. Wu, M. Zhou and B. Hu, Microporous Mesoporous Mater., 2016, 234, 230-238.
207. K. Ma, J. Cheng, J. Zhang, M. Li, F. Liu and X. Zhang, Electrochim. Acta, 2016, 198, 231-240.
208. M. A. Woo, M.-S. Song, T. W. Kim, I. Y. Kim, J.-Y. Ju, Y. S. Lee, S. J. Kim, J.-H. Choy and S.-J. Hwang, J. Mater. Chem., 2011, 21, 4286-4292.
209. J. Gou, S. Xie, Y. Liu and C. Liu, Electrochim. Acta, 2016, 210, 915-924.
210. L. Qian, Z. Lu, T. Xu, X. Wu, Y. Tian, Y. Li, Z. Huo, X. Sun and X. Duan, Advanced Energy Materials, 2015, 5.
211. Q. Liu, H. Wang, X. Wang, R. Tong, X. Zhou, X. Peng, H. Wang, H. Tao and Z. Zhang, Int. J. Hydrogen Energy, 2017, 42, 5560-5568.
212. P. Li, Q. Xie, L. Zheng, G. Feng, Y. Li, Z. Cai, Y. Bi, Y. Li, Y. Kuang and X. Sun, Nano Research, 2017, 10, 2988-2997.
213. X.-Y. Yu, T. Luo, Y. Jia, R.-X. Xu, C. Gao, Y.-X. Zhang, J.-H. Liu and X.-J. Huang, Nanoscale, 2012, 4, 3466-3474.
214. Y. Sun, S. Gao and Y. Xie, Chem. Soc. Rev., 2014, 43, 530-546.

215. Y. Zhao, G. Chen, T. Bian, C. Zhou, G. I. Waterhouse, L. Z. Wu, C. H. Tung, L. J. Smith, D. O'Hare and T. Zhang, Adv. Mater. , 2015, 27, 7824-7831.
216. Y. Zhao, Y. Zhao, G. I. Waterhouse, L. Zheng, X. Cao, F. Teng, L. Z. Wu, C. H. Tung, D. O'Hare and T. Zhang, Adv. Mater. , 2017.
217. J. Yu, B. R. Martin, A. Clearfield, Z. Luo and L. Sun, Nanoscale, 2015, 7, 9448-9451.
218. J. Yu, J. Liu, A. Clearfield, J. E. Sims, M. T. Speiegle, S. L. Suib and L. Sun, Inorg. Chem., 2016, 55, 12036-12041.
219. Y. Zhao, Y. Zhao, G. I. N. Waterhouse, L. Zheng, X. Cao, F. Teng, L.-Z. Wu, C.-H. Tung, D. O'Hare and T. Zhang, Advanced materials (Deerfield Beach, Fla.), 2017, DOI: 10.1002/adma.201703828.
220. Y. Sun, S. Gao, F. Lei, C. Xiao and Y. Xie, Acc. Chem. Res., 2014, 48, 3-12.
221. F. Song and X. Hu, Nature communications, 2014, 5.
222. P. Sun, R. Ma, X. Bai, K. Wang, H. Zhu and T. Sasaki, Science Advances, 2017, 3, e1602629.
223. G. Hu, N. Wang, D. O'Hare and J. Davis, J. Mater. Chem., 2007, 17, 2257-2266.
224. G. Hu and D. O'Hare, J. Am. Chem. Soc., 2005, 127, 17808-17813.
225. Q. Wang, S. V. Y. Tang, E. Lester and D. O'Hare, Nanoscale, 2013, 5, 114-117.
226. V. Nicolosi, M. Chhowalla, M. G. Kanatzidis, M. S. Strano and J. N. Coleman, Science, 2013, 340, 1226419.
227. H. Liang, F. Meng, M. CabГЎn-Acevedo, L. Li, A. Forticaux, L. Xiu, Z. Wang and S. Jin, Nano Lett., 2015, 15, 1421.
228. Z. Lu, W. Xu, W. Zhu, Q. Yang, X. Lei, J. Liu, Y. Li, X. Sun and X. Duan, Chem. Commun., 2014, 50, 6479-6482.
229. T. Li, G. Li, L. Li, L. Liu, Y. Xu, H. Ding and T. Zhang, ACS Appl. Mat. Interfaces 2016, 8, 2562-2572.
230. H. Li, Z. Chen, Y. Wang, J. Zhang and X. Yan, Electrochim. Acta, 2016, 210, 15-22.
231. T. Li, R. Li and H. Luo, Journal of Materials Chemistry A, 2016, 4, 18922-18930.
232. K. Dutta and A. Pramanik, Chem. Commun., 2013, 49, 6427-6429.
233. M. Yang, J. Liu, Z. Chang, G. R. Williams, D. O'Hare, X. Zheng, X. Sun and X. Duan, J. Mater. Chem., 2011, 21, 14741-14746.
234. W. Lv, M. Du, W. Ye and Q. Zheng, Journal of Materials Chemistry A, 2015, 3, 23395-23402.
235. C. J. Wang and D. O'Hare, J. Mater. Chem., 2012, 22, 23064-23070.
236. L. Chen, C. Li, Y. Wei, G. Zhou, A. Pan, W. Wei and B. Huang, J. Alloys Compd., 2016, 687, 499-505.
237. M. Shao, F. Ning, J. Zhao, M. Wei, D. G. Evans and X. Duan, Adv. Funct. Mater., 2013, 23, 3513-3518.
238. Z. Li, B. Yang, S. Zhang, B. Wang and B. Xue, Journal of Materials Chemistry A, 2014, 2, 10202-10210.
239. T. Zhang, Z. Mei, Y. Zhou, X. Bu, Y. Wang, Q. Li and X. Yang, CrystEngComm, 2014, 16, 1793-1801.
240. L. Li, R. Ma, N. Iyi, Y. Ebina, K. Takada and T. Sasaki, Chem. Commun., 2006, 3125-3127.
241. C. Zhang, M. Shao, L. Zhou, Z. Li, K. Xiao and M. Wei, ACS Appl. Mat. Interfaces 2016, 8, 33697-33703.
242. E. Géraud, S. Rafqah, M. Sarakha, C. Forano, V. Prevot and F. Leroux, Chem. Mater., 2007, 20, 1116-1125.
243. P. G. Rodriguez, M. de Ruiter, T. Wijnands and J. Ten Elshof, Scientific reports, 2017, 7.
244. N. Abushrenta, X. Wu, J. Wang, J. Liu and X. Sun, Scientific reports, 2015, 5.
245. P. F. Liu, S. Yang, B. Zhang and H. G. Yang, ACS Appl. Mat. Interfaces 2016, 8, 34474-34481.
246. Y. Sun, Q. Liu, S. Gao, H. Cheng, F. Lei, Z. Sun, Y. Jiang, H. Su, S. Wei and Y. Xie, Nature communications, 2013, 4, 2899.
247. M. Zubair, M. Daud, G. McKay, F. Shehzad and M. A. Al-Harthi, Appl. Clay Sci., 2017, 143, 279-292.
248. G. Fan, F. Li, D. G. Evans and X. Duan, Chem. Soc. Rev., 2014, 43, 7040-7066.
249. S. M. Shaheen, N. K. Niazi, N. E. Hassan, I. Bibi, H. Wang, D. C. Tsang, Y. S. Ok, N. Bolan and J. Rinklebe, Int. Mater. Rev., 2019, 64, 216-247.
250. M. González, I. Pavlovic, R. Rojas-Delgado and C. Barriga, Chem. Eng. J., 2014, 254, 605-611.
251. H. Asiabi, Y. Yamini and M. Shamsayei, J. Hazard. Mater., 2017, 339, 239-247.
252. M. W. Laipan, H. Y. Fu, R. L. Zhu, L. Y. Sun, R. M. Steel, S. J. Ye, J. X. Zhu and H. P. He, Appl. Clay Sci., 2018, 153, 46-53.
253. J. Gong, T. Liu, X. Wang, X. Hu and L. Zhang, Environ. Sci. Technol., 2011, 45, 6181-6187.
254. T. Wen, X. Wu, X. Tan, X. Wang and A. Xu, ACS Appl. Mat. Interfaces 2013, 5, 3304-3311.
255. G. B. B. B. Varadwaj, O. A. Oyetade, S. Rana, B. S. Martincigh, S. B. Jonnalagadda and V. O. Nyamori, ACS Appl. Mat. Interfaces 2017.
256. G. Sheng, J. Hu, H. Li, J. Li and Y. Huang, Chemosphere, 2016, 148, 227-232.
257. B. Zhang, L. Luan, R. Gao, F. Li, Y. Li and T. Wu, Colloids Surf., A 2017, 520, 399-408.
258. S. U. Nandanwar, K. Coldsnow, V. Utgikar, P. Sabharwall and D. E. Aston, Chem. Eng. J., 2016, 306, 369-381.
259. X. Zhang, J. Wang, R. Li, Q. Dai, R. Gao, Q. Liu and M. Zhang, Ind. Eng. Chem. Res., 2013, 52, 10152-10159.
260. L. Tan, Y. Wang, Q. Liu, J. Wang, X. Jing, L. Liu, J. Liu and D. Song, Chem. Eng. J., 2015, 259, 752-760.
261. G. Sheng, Y. Tang, W. Linghu, L. Wang, J. Li, H. Li, X. Wang and Y. Huang, Appl. Catal., B 2016, 192, 268-276.
262. W. Linghu, H. Yang, Y. Sun, G. Sheng and Y. Huang, ACS Sustainable Chemistry & Engineering, 2017.
263. Y. Zou, Y. Liu, X. Wang, G. Sheng, S. Wang, Y. Ai, Y. Ji, Y. Liu, T. Hayat and X. Wang, ACS Sustainable Chemistry & Engineering, 2017, 5, 3583-3595.
264. W. Yao, X. Wang, Y. Liang, S. Yu, P. Gu, Y. Sun, C. Xu, J. Chen, T. Hayat and A. Alsaedi, Chem. Eng. J., 2018, 332, 775-786.
265. Y. Zou, P. Wang, W. Yao, X. Wang, Y. Liu, D. Yang, L. Wang, J. Hou, A. Alsaedi and T. Hayat, Chem. Eng. J., 2017, 330, 573-584.
266. T. G. Levitskaia, S. Chatterjee, B. W. Arey, E. L. Campbell, Y. Hong, L. Kovarik, J. M. Peterson, N. K. Pence, J. Romero and V. Shutthanandan, RSC Advances, 2016, 6, 76042-76055.
267. D. Banerjee, D. Kim, M. J. Schweiger, A. A. Kruger and P. K. Thallapally, Chem. Soc. Rev., 2016, 45, 2724-2739.
268. M. Zhang, Q. Yao, C. Lu, Z. Li and W. Wang, ACS Appl. Mat. Interfaces 2014, 6, 20225-20233.
269. P. Zhao, X. Liu, W. Tian, D. Yan, X. Sun and X. Lei, Chem. Eng. J., 2015, 279, 597-604.
270. S. Yu, X. Wang, Z. Chen, J. Wang, S. Wang, T. Hayat and X.


 

Wang, J. Hazard. Mater., 2017, 321, 111-120.
271. D. Bharali and R. C. Deka, Colloids Surf., A 2017, 525, 64-76.
272. X. Yue, J. Li, T. Zhang, F. Qiu, D. Yang and M. Xue, Chem. Eng. J., 2017, 328, 117-123.
273. G. Carja, E. F. Grosu, M. Mureseanu and D. Lutic, Catalysis Science & Technology, 2017.
274. Y. Meng, W. Luo, S. Xia and Z. Ni, Catalysts, 2017, 7, 143.
275. J. Yuan, X. Liu, O. Akbulut, J. Hu, S. L. Suib, J. Kong and F. Stellacci, Nat. Nanotechnol., 2008, 3, 332-336.
276. Q. Wang, G. Chen, J. Tian, Z. Yu, Q. Deng and M. Yu, Mater. Lett., 2018, 230, 84-87.
277. Q. Wang, M. Yu, G. Chen, Q. Chen and J. Tian, J. Mater. Sci., 2017, 52, 2549-2559.
278. Q. Wang, M. Yu, G. Chen, Q. Chen and J. Tai, BioResources, 2017, 12, 643-654.
279. Q. Wang, J. Xiong, G. Chen, O. Xinping, Z. Yu, Q. Chen and M. Yu, Materials, 2019, 12, 1393.
280. Y. Lin, P. Yi, M. Yu and G. Li, Mater. Lett., 2018, 230, 219-223.
281. X. Liu, L. Ge, W. Li, X. Wang and F. Li, ACS Appl. Mat. Interfaces 2014, 7, 791-800.
282. S. S. Elanchezhiyan and S. Meenakshi, Int. J. Biol. Macromol., 2017.
283. J. Luo, W. Zhang, H. Yuan, C. Jin, L. Zhang, H. Huang, C. Liang, Y. Xia, J. Zhang and Y. Gan, ACS Nano, 2017, 11, 2459-2469.
284. C. Eames and M. S. Islam, J. Am. Chem. Soc., 2014, 136, 16270-16276.
285. G. G. Yadav, J. W. Gallaway, D. E. Turney, M. Nyce, J. Huang, X. Wei and S. Banerjee, Nature Communications, 2017, 8.
286. J. Zhang, Z. Zhang, Y. Yao, X. Ma, Y. Yang, Y. Chen and Z. Cheng, Appl. Surf. Sci., 2019.
287. C. Peng, P. Wei, X. Li, Y. Liu, Y. Cao, H. Wang, H. Yu, F. Peng, L. Zhang and B. Zhang, Nano energy, 2018, 53, 97-107.
288. B. G. Pollet, I. Staffell and J. L. Shang, Electrochim. Acta, 2012, 84, 235-249.
289. X. Luo, Q. Zhou, S. Du, J. Li, L. Zhang, K. Lin, H. Li, B. Chen, T. Wu and D. Chen, ACS Appl. Mat. Interfaces 2018, 10, 42335-42347.
290. X. Long, Z. Wang, S. Xiao, Y. An and S. Yang, Mater. Today 2016, 19, 213-226.
291. Y. Jia, L. Zhang, G. Gao, H. Chen, B. Wang, J. Zhou, M. T. Soo, M. Hong, X. Yan and G. Qian, Adv. Mater. , 2017, 29.
292. G. Hatui, G. C. Nayak and G. Udayabhanu, Electrochim. Acta, 2016, 219, 214-226.
293. P. Simon and Y. Gogotsi, Nat. Mater., 2008, 7, 845-854.
294. J. Han, Y. Ping, J. Li, Z. Liu, B. Xiong, P. Fang and C. He, Diamond Relat. Mater., 2019, 96, 176-181.
295. Q. Zhou, T. Fan, Y. Li, D. Chen, S. Liu and X. Li, J. Power Sources, 2019, 426, 111-115.
296. S. Zhang, C. Wu, W. Wu, C. Zhou, Z. Xi, Y. Deng, X. Wang, P. Quan, X. Li and Y. Luo, J. Power Sources, 2019, 424, 1-7.
297. M. Yao, X. Zhao, J. Zhang, W. Tan, J. Luo, J. Dong and Q. Zhang, Nanotechnology, 2018, 30, 085404.
298. P. Ou, Q. Zhou, J. Li, W. Chen, J. Huang, L. Yang, J. Liao and M. Sheng, Materials Research Express, 2019, 6, 095044.
299. C. Tan, X. Cao, X.-J. Wu, Q. He, J. Yang, X. Zhang, J. Chen, W. Zhao, S. Han and G.-H. Nam, Chem. Rev., 2017, 117, 6225-6331.
300. J. Yang, C. Yu, X. Fan and J. Qiu, Adv. Energy Mater., 2014, 4, 1400761.
301. B. Zhu, G. Guo, G. Wu, Y. Zhang, A. Dong, J. Hu and D. Yang, J. Alloys Compd., 2019, 775, 776-783.
302. F. Wang, C. Wang, H. Chen, W. Zhang, R. Jiang, Z. Yan, Z. Huang, H. Zhou and Y. Kuang, Nanotechnology, 2019, 30, 335701.
303. P. Liang, L. Zhang, D. Wang, X. Man, H. Shu, L. Wang, H. Wan, X. Du and H. Wang, Appl. Surf. Sci., 2019.
304. Q. Wang, L. Shang, R. Shi, X. Zhang, Y. Zhao, G. I. Waterhouse, L. Z. Wu, C. H. Tung and T. Zhang, Advanced Energy Materials, 2017, 7.
305. Z. Yan, E. Wang, J. Gao, J. Yang, C. Wu, L. Jiang, M. Zhu and G. Sun, ChemElectroChem.
306. A. Flegler, S. Müssig, J. Prieschl, K. Mandel and G. Sextl, Electrochim. Acta, 2017, 231, 216-222.
307. J. Zhang, H. Hu, Z. Li and X. W. D. Lou, Angew. Chem. Int. Ed. , 2016, 55, 3982-3986.
308. P. G. Bruce, S. A. Freunberger, L. J. Hardwick and J.-M. Tarascon, Nat. Mater., 2012, 11, 19-29.
309. X. Ji and L. F. Nazar, J. Mater. Chem., 2010, 20, 9821-9826.
310. A. Manthiram, Y. Fu, S.-H. Chung, C. Zu and Y.-S. Su, Chem. Rev., 2014, 114, 11751-11787.
311. S. Evers and L. F. Nazar, Acc. Chem. Res., 2012, 46, 1135-1143.
312. X. Wen, Z. Yang, X. Xie, Z. Feng and J. Huang, Electrochim. Acta, 2015, 180, 451-459.
313. Y. Liu and Z. Yang, RSC Advances, 2016, 6, 68584-68591.
314. J. Long, Z. Yang, J. Huang and X. Zeng, J. Power Sources, 2017, 359, 111-118.
315. X. Zeng, Z. Yang, F. Liu, J. Long, Z. Feng and M. Fan, RSC Advances, 2017, 7, 44514-44522.
316. M. Bastianini, R. Vivani, M. Nocchetti, D. Costenaro, C. Bisio, F. Oswald, T. B. Meyer and L. Marchese, Sol. Energy 2014, 107, 692-699.
317. J. H. Lee, J. Chang, J. H. Cha, D. Y. Jung, S. S. Kim and J. M. Kim, Chemistry-A European Journal, 2010, 16, 8296-8299.
318. X. Wang, R. Deng, S. A. Kulkarni, X. Wang, S. S. Pramana, C. C. Wong, M. Grätzel, S. Uchida and S. G. Mhaisalkar, Journal of Materials Chemistry A, 2013, 1, 4345-4351.
319. T. Du, J. Zhu, N. Wang, H. Chen and H. He, J. Electrochem. Soc., 2015, 162, H518-H521.
320. C. Li, M. Wei, D. G. Evans and X. Duan, Small, 2014, 10, 4469-4486.
321. M. Luo, Z. Cai, C. Wang, Y. Bi, L. Qian, Y. Hao, L. Li, Y. Kuang, Y. Li and X. Lei, Nano Research, 2017, 10, 1732-1739.
322. X. Li, X. Hao, Z. Wang, A. Abudula and G. Guan, J. Power Sources, 2017, 347, 193-200.
323. N. Han, F. Zhao and Y. Li, Journal of Materials Chemistry A, 2015, 3, 16348-16353.
324. X. Long, J. Li, S. Xiao, K. Yan, Z. Wang, H. Chen and S. Yang, Angew. Chem., 2014, 126, 7714-7718.
325. M. Wang, M. Shen, L. Zhang, J. Tian, X. Jin, Y. Zhou and J. Shi, Carbon, 2017, 120, 23-31.
326. S. He, Z. An, M. Wei, D. G. Evans and X. Duan, Chem. Commun., 2013, 49, 5912-5920.
327. Y. Kuthati, R. K. Kankala and C.-H. Lee, Appl. Clay Sci.,

2015, 112, 100-116.
328. P. Wang, J. Wang, H. Tan, S. Weng, L. Cheng, Z. Zhou and S. Wen, Biomaterials science, 2018, 6, 1262-1270.
329. A. Díaz, A. David, R. Pérez, M. L. González, A. Báez, S. E. Wark, P. Zhang, A. Clearfield and J. L. Colón, Biomacromolecules, 2010, 11, 2465-2470.
330. Y. Zhang, M. Long, P. Huang, H. Yang, S. Chang, Y. Hu, A. Tang and L. Mao, Nano Research, 2017, 1-11.
331. T. Xu, J. Zhang, H. Chi and F. Cao, Acta Biomater., 2016, 36, 152-163.
332. S. T. Frey, S. L. Guilmet, R. G. Egan III, A. Bennett, S. R. Soltau and R. C. Holz, ACS Appl. Mat. Interfaces 2010, 2, 2828-2832.
333. A. Li, L. Qin, D. Zhu, R. Zhu, J. Sun and S. Wang, Biomaterials, 2010, 31, 748-756.
334. G. Mishra, B. Dash and S. Pandey, Appl. Clay Sci., 2018, 153, 172-186.
335. A. Li, L. Qin, W. Wang, R. Zhu, Y. Yu, H. Liu and S. Wang, Biomaterials, 2011, 32, 469-477.
336. J.-H. Choy, S.-J. Choi, J.-M. Oh and T. Park, Appl. Clay Sci., 2007, 36, 122-132.
337. S.-J. Choi and J.-H. Choy, Nanomedicine, 2011, 6, 803-814.
338. L.-x. Zhang, X.-x. Xie, D.-q. Liu, Z. P. Xu and R.-t. Liu, Biomaterials, 2018, 174, 54-66.
339. A. U. Kura, S. H. H. Al Ali, M. Z. Hussein, S. Fakurazi and P. Arulselvan, Int. J. Nanomedicine, 2013, 8, 1103.
340. G. Kapusetti, N. Misra, V. Singh, R. Kushwaha and P. Maiti, Journal of Biomedical Materials Research Part A, 2012, 100, 3363-3373.
341. C. Chen, P. Gunawan, X. W. Lou and R. Xu, Adv. Funct. Mater., 2012, 22, 780-787.
342. F. Peng, D. Wang, D. Zhang, H. Cao and X. Liu, Appl. Clay Sci., 2018, 165, 179-187.
343. Y.-M. Kuo, Y. Kuthati, R. K. Kankala, P.-R. Wei, C.-F. Weng, C.-L. Liu, P.-J. Sung, C.-Y. Mou and C.-H. Lee, Journal of Materials Chemistry B, 2015, 3, 3447-3458.
344. Z. Li, H. Duan, M. Shao, J. Li, D. O'Hare, M. Wei and Z. L. Wang, Chem, 2018, 4, 2168-2179.

ARTICLE

## Table of contents entry

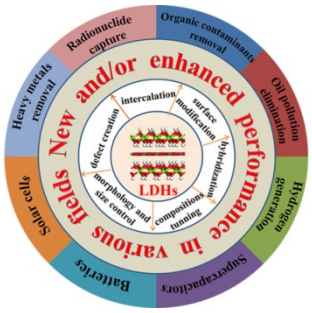


Functionalization strategies are powerful for generating new or enhanced properties of LDHs, offering unique perspectives and advantages for preparing novel materials.